QUICK METHODS OF ANALYSING EARTHQUAKE FORCES ON VIADUCT BRIDGES HAVING CONTINUOUS DECKS AND TALL PIERS

by

I. G. STRICKLAND

A thesis submitted in partial fulfilment
of the requirements for the degree
Master of Science in Engineering

Department of Civil Engineering
UNIVERSITY OF CAPE TOWN

APRIL 1980

ACKNOWLEDGEMENTS

The subject of this thesis arose from design work being done in the offices of Messrs. Watermeyer, Legge, Piesold and Uhlmann, whose support is gratefully acknowledged.

Professor J.B. Martin, who supervised this work, is gratefully thanked for his valued guidance and advice. Mr. B. Mackenzie's comments and Mr. G. Howell's assistance in mobilizing the S.A.P. IV computer programme are greatly appreciated.

I am indebted to Mrs. W. Didcock for doing most of the typing.

TABLE OF CONTENTS

TABLE OF CONTENTS

(Continued)

TABLE OF CONTENTS

(Continued)

LIST OF FIGURES

LIST OF FIGURES

(Continued)

LIST OF TABLES

LIST OF TABLES

(Continued)

SYNOPSIS

The available methods of calculating the effects of earthquakes on viaduct-type bridges with continuous decks and tall piers are examined. Particular emphasis is laid on the use of a relatively quick method of analysis using response spectra and taking account of the effects of damping.

The use of this method is illustrated by applying it to a mathematical model representing a real bridge. Manual calculations are performed and refined by the application of Rayleigh's Principle.

A number of variations to the configuration of the model are analysed by the computer programme "SAP IV" under earthquake excitation in each of three mutually perpendicular directions. The computed results are compared with those obtained by manual calculation.

The earthquake loading effects are compared with the effects of deadload, traffic loading and windload and there is a discussion on the design of suitable structural configurations to contend with seismic loading. The work ends with some generalisations about other types of bridges.

CHAPTER 1

AIM OF THESIS

The aim of this thesis is to examine the available methods of calculating the effects of earthquakes on viaduct-type bridges with continuous decks and tall piers. In particular the thesis seeks to illustrate the value of relatively quick methods of determining the effects of various structural configurations so that the designer of a particular structure can converge upon the optimum configuration before resorting to rigorous analyses requiring time-consuming and costly computer runs. The scope of this thesis does not permit the inclusion of all the effects that an earthquake could have on a structure of this type. Accordingly, the main emphasis of the work lies in the interaction of the piers and the deck with idealised assumptions for founding conditions.

The mathematical model used for illustrating the effects of parameter changes is a simplified representation of a bridge which is being designed in the offices of the writer.

CHAPTER 2

GROUND MOVEMENTS AND STRUCTURAL RESPONSE

Much has been written about and much controversy surrounds the causes of earthquakes. B.A. Bolt[1] states that we are interested only in the classes of earthquake in which there is a release of energy near to the earth's surface and large enough to cause damage to structures. Most earthquakes of engineering significance are caused by the sudden relative displacements of the rock on the two sides of a fault plane. The stress waves resulting from the sudden release of strain energy radiate from the source through the rock mass in a manner which is non-uniform and depends upon the elastic properties of the rock or ground through which the waves are propagated.

At any particular point remote from the source, the ground movements felt will be superimposed effects of pulses arriving at that point via different routes. The cumulative effect will be a non periodic and random shaking of the ground in which the amplitude and frequency of oscillations are irregular. The motion will normally have both horizontal and vertical components.

It is most convenient to record earthquakes by measuring the accelerations of the ground vertically and in 2 mutually perpendicular horizontal directions. These are plotted by the recording instrument on an accelerogram. The velocity and displacement curves can then be derived from the accelerogram by integration with time. Housner[2] observes that in most earthquakes the vertical ground acceleration is one-third to two-thirds as intense as the horizontal acceleration and has higher frequency components.

When a structure is subjected to an earthquake, its foundations are forced to undergo the movements of the ground or rock upon which they are built. The manner in which the structure responds to a given set of movements of its found-

ations varies considerably from one structure to another and depends upon a number of structural parameters, such as :

1. The stiffness of the structural components.

2. The mass of the structural components.

3. Whether the structural deformations remain elastic or enter the inelastic range.

4. The capacity of the structure to resist alterations to its configuration; e.g. irreversible displacement of superstructure relative to substructure due to damaged bearings.

CHAPTER 3

THE NEED FOR EARTHQUAKE DESIGN OF STRUCTURES IN SOUTH AFRICA

The occurrence of the earthquake which caused severe damage in Tulbagh/Ceres area in September 1969 and the one which destroyed a block of flats in Welkom more recently, have served to make designers more conscious of the possibility of further seismic events which could affect the safety of their designs.

Although South Africa is generally considered a fairly stable region as far as earthquakes are concerned, Laurie and Putterill[3] have pointed out that South Africa experiences, on average, about 30 earthquakes per year. They state further: "Although the major earthquake at Ceres occurred in a region of known geological faulting, the fault has not been considered an active one and it is understood from seismologists that the occurrence of the earthquake cannot be considered as presaging an era of increased seismic activity in the area. It seems that the next severe earthquake could equally readily occur in some other part of the country ....."

The bridge which the writer is studying spans a valley which is crossed by a number of faults that are regarded as being inactive. Considering that the geological faulting at Ceres was also regarded as inactive it would seem equally possible that an earthquake of similar magnitude could occur at the bridge site. The Ceres earthquake had a Richter magnitude of 6,5. The focal depth was shallow and the epicentre was apparently just north of Tulbagh. The intensity on the Modified Mercalli scale varied between VII to VIII in the towns of Tulbagh, Ceres and Wolseley. This intensity would be associated with a maximum ground acceleration of approximately 0,1g. The intensity at the epicentre would probably have been close to IX with a corresponding ground acceleration of the order of 0,3g.

TABLE 3.1 *Approximate correspondence between Richter magnitude, Modified Mercalli intensity, maximum ground acceleration and radius of perceptibility of earthquakes under average conditions* (Ref. 3)

Richter magnitude M	Modified Mercalli intensity at epicentre MM	Max. ground acceleration at epicentre	Approx. radius of perceptibility
3	II – III	0.003g	25 km
4	IV – V	0.01g	50 km
5	VI	0.03g	100 km
6	VII – VIII	0.1g	200 km
7	IX	0.3g	400 km
8	X – XI	1g	700 km

g = gravitational acceleration

CHAPTER 4

RESULTS REQUIRED FROM EARTHQUAKE ANALYSIS

An earthquake will impose certain inertia loads on the structure and the effects thereof must be considered in conjunction with other load cases such as the dead load, the applied live loading, wind loading and temperature effects.

The method of seismic analysis to be used will be affected by whether or not the structure undergoes permanent non-linear deformations and fractures. In either event, the displacements, moments and forces in various parts of the structure will be required. The displacements are of interest when determining the range of movements to be accommodated by bearings and expansion joints whilst the moments and forces are required in strength calculations.

In certain cases the natural frequency of oscillation of the structure in some of the lower modes is of interest in order to check that it does not coincide with any anticipated cyclic loading with the same frequency.

Within the scope of this thesis only linear deformations will be considered.

CHAPTER 5

EQUATIONS OF MOTION

The inertia forces acting on any part of a structure depend on the mass of that part and the acceleration to which it is subjected. Very little accuracy is lost if the mass of the structure is considered to be lumped at judiciously selected discrete points. The motion of the structure during oscillation is described in terms of the displacements of the points at which the masses are lumped. The number of displacement components needed to specify the position of all lumped mass points is called the number of "degrees of freedom" of the structure. For example, the systems shown in figure 5.1 have only one degree of freedom, v_1, whereas the vertical cantilever shown in figure 5.2 has 3 degrees of freedom, v_1, v_2 and v_3.

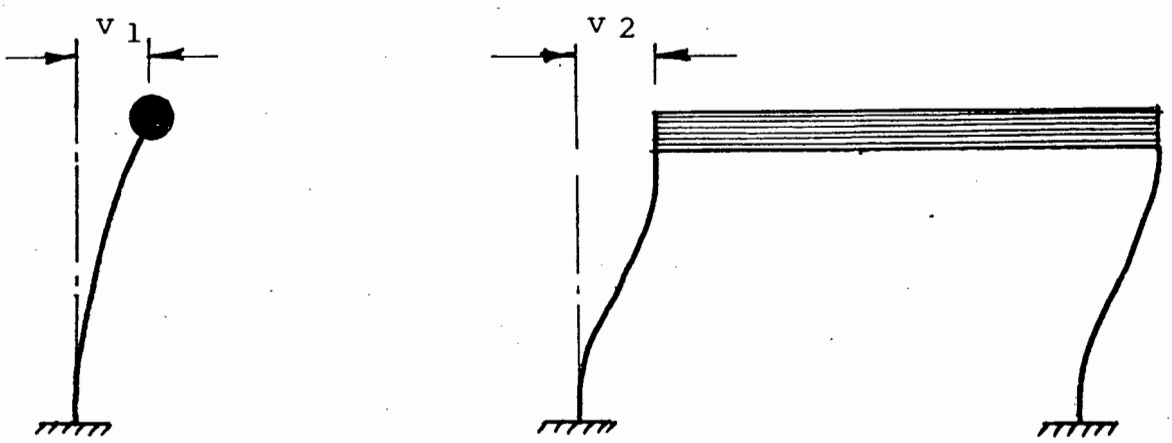

FIGURE 5.1 : SINGLE-DEGREE-OF-FREEDOM SYSTEMS

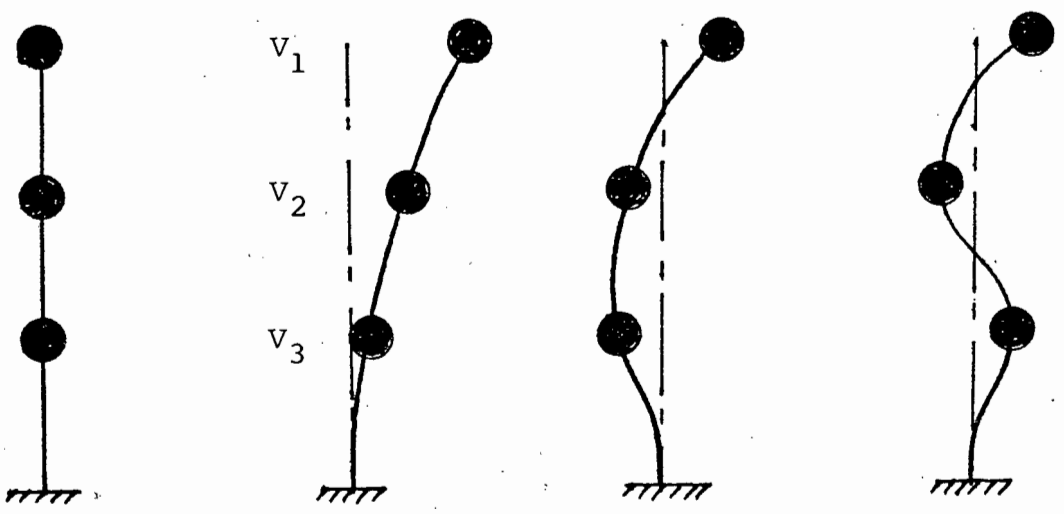

FIGURE 5.2 : MODES OF OSCILLATION FOR VERTICAL CANTILEVER HAVING 3 DEGREES OF FREEDOM

There are 3 possible basic shapes into which the system shown in figure 5.2 can deform during oscillation and each of these shapes is called a "mode". A system with more than one degree of freedom is called a multi degree of freedom system. In such a system the modes of oscillation are independent of each other. Any number of the possible modes may act at any one time, the effects being superimposed. There are always as many modes of oscillation as there are degrees of freedom.

For any particular system, each mode is associated with its own natural period of oscillation which does not vary. The mode shapes and natural periods are characteristics of the system and are independent of the earthquake. For each degree of freedom there will be a mode of vibration and the equations of motion of that mode express the dynamic equilibrium of all the forces acting on the structure. Figure 5.3 shows a typical single-degree-of-freedom structure consisting of an infinitely stiff beam resting upon flexible columns.

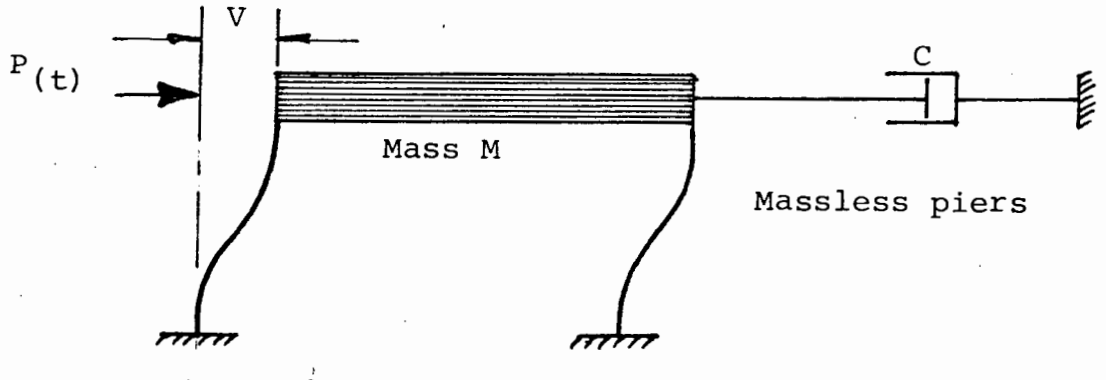

Fig. 5.3 Typical Single-degree-of-freedom Structure

The system has only one effective degree of freedom which is horizontal displacement of the beam. There is assumed to be a damping force which resists motion with a force proportional to the velocity. The stiffness of the supports is taken to be the force required to produce unit displacement.

For equilibrium during vibration

$$F_I + F_D + F_s = P_{(t)} \tag{5.1}$$

in which

$P_{(t)}$ = externally applied force at time t
F_I = Inertia force
F_D = Damping force
F_s = Elastic force

The inertia force F_I = mass x acceleration

$$= M\ddot{v} \tag{5.2}$$

The damping force F_D = damping coefficient x velocity

$$= C\dot{v} \tag{5.3}$$

The elastic force F_S = column stiffness x displacement

$$= Kv \tag{5.4}$$

Substituting in eqn. (5.1)

$$M\ddot{v} + C\dot{v} + Kv = P_{(t)} \tag{5.5}$$

For a response induced by an earthquake, there is no externally applied load, thus $P_{(t)} = 0$.

$$\therefore \quad M\ddot{v} + C\dot{v} + Kv = 0 \tag{5.6}$$

This is the condition known as free vibration. In the case where there is no damping, C = 0 and eqn. (5.6) becomes:

$$M\ddot{v} + K\dot{v} = 0$$

$$\text{i.e} \quad \ddot{v} + \frac{Kv}{M} = 0 \tag{5.7}$$

If we put $\frac{K}{M} = \omega^2$ then

$$\ddot{v} + \omega^2 v = 0 \qquad (5.8)$$

The solution of the differential equation (5.8) is given by the equation of simple harmonic motion.

$$v = A \sin \omega t + B \cos \omega t \qquad (5.9)$$

in which A and B are constants

Let v_o = initial displacement and $\dot{v}_o$ = initial velocity.

Differentiating eqn. (5.8)

$$\dot{v} = \omega A \cos \omega t - \omega B \sin \omega t \qquad (5.10)$$

When $t = 0$, $v = v_o$ and $\dot{v} = \dot{v}_o$

$$\therefore v_o = A \sin 0 + B \cos 0 \qquad (5.11)$$

$$\therefore B = v_o$$

and $\dot{v}_o = \omega A \cos 0 - \omega B \sin 0$

$$\therefore \dot{v}_o = \omega A$$

$$\therefore A = \frac{\dot{v}_o}{\omega} \qquad (5.12)$$

Substituting for A and B in eqn. (5.9)

$$v = \frac{\dot{v}_o}{\omega} \sin \omega t + v_o \cos \omega t \qquad (5.13)$$

This solution may be verified by differentiating the displacment to obtain velocity and the velocity to obtain the acceleration.

$$\dot{v} = \dot{v}_o \cos \omega t - \omega v_o \sin \omega t$$

and $\ddot{v} = -\omega \dot{v}_o \sin \omega t - \omega^2 v_o \cos \omega t$

i.e $\ddot{v} = -\omega^2 \left(\frac{\dot{v}_o}{\omega} \sin \omega t + v_o \cos \omega t\right)$

$= -\omega^2 v$

i.e $\ddot{v} + \omega^2 v = 0$

This is a restatement of eqn. (5.8)

If t is measured from the instant of an extreme position, $\dot{v}_o = 0$ and $v_o = v$ max.

Substituting in eqn. (5.13),

$$v = v \text{ max } \cos\omega t \qquad (5.14)$$

This motion is illustrated in figure 5.4.

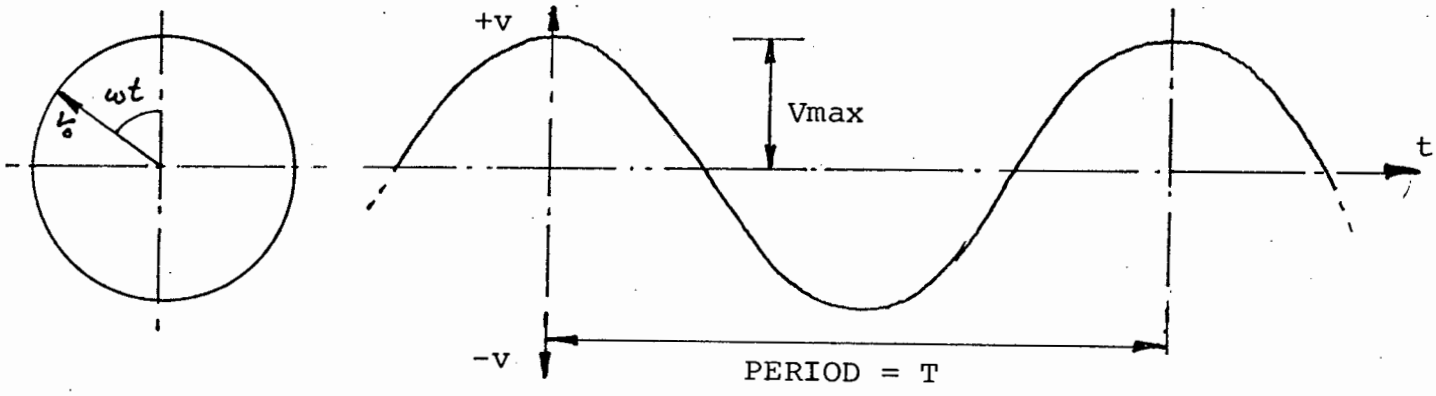

Fig. 5.4 Graphical representation of the motion v = Vmax cos ωt

To determine the period, ωt = 1 full revolution

$$= 2\pi$$

$$\therefore \quad t = \frac{2\pi}{\omega} = T \qquad (5.15)$$

Since $\omega = \sqrt{\frac{K}{M}}$

$$\therefore \quad T = 2\pi\sqrt{\frac{M}{K}} \qquad (5.16)$$

It is noteworthy that T is independent of the amplitude of vibration and can be obtained from a knowledge of the mass and the stiffness of the structure.

CHAPTER 6

COMPUTATION OF LINEAR ELASTIC RESPONSES

6.1 Time-History Analysis

During an earthquake the shaking of the ground at any particular point may endure for periods which are typically from 10 to 30 seconds. During this period the ground will undergo many oscillations of varying amplitude and frequency as represented by an accelerogram.

The response of a structure to this type of ground motion requires the application of the equationsof motion to the structure for each time step in a series of equal time steps covering the duration of the ground motion. For each time step, the changes to the displacements and the velocities are computed and added to the displacements and velocities computed at the end of the previous time step. A number of different methods of performing this integration have been developed.

By this process of integration a history of the displacements, moments and forces for the full duration of the earthquake may be built up.

A typical accelerogram is shown in figure 6.1

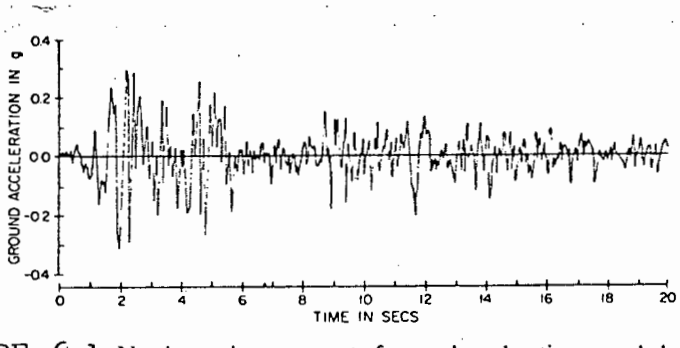

FIGURE 6.1 North–south component of ground acceleration recorded at El Centro approximately 4 mi from the causative fault of the magnitude 7.1, May 18, 1940, earthquake. Recorded on very deep (5000+ ft) alluvium with ground water close to the surface. Ref. 1.2

In order to preserve acceptable accuracy the length of each time step has to be very small. In some preliminary computations for the bridge, a time step of 0,00035 seconds was used. For each of these time intervals a complete load case is analysed and, as a result, the large amount of computation takes time and becomes expensive.

6.2 Response Spectrum Analysis

If a simple oscillator, being a single degree of freedom system with a particular natural period, is subjected to a particular earthquake, as represented by its accelerogram, then the history of its response motion can be computed by direct integration as described in 6.1. From such an analysis the maximum values of acceleration, pseudo-velocity and displacement attained by the oscillator during the earthquake may be extracted. If D is the maximum displacement of the oscillating mass relative to the ground and K is the stiffness of the system, the pseudo-velocity V is defined as a quantity having the dimensions of velocity such that the energy stored in the system can be expressed by the equation

$$\tfrac{1}{2}KD^2 = \tfrac{1}{2}MV^2 \qquad (6.1)$$

from which

$$V = \sqrt{\frac{K}{M}}\, D \qquad (6.2)$$

From equation (5.8), $\frac{K}{M} = \omega^2$

Substituting in equation (6.2)

$$V = \omega D \qquad (6.3)$$

From equation (5.8) acceleration $= \omega^2$ x displacement, from which pseudoacceleration $Ag = \omega^2 D$

where g = acceleration due to gravity.

The pseudovelocity V is nearly equal to the maximum relative velocity for systems with moderate or high frequencies but may differ considerably from the maximum relative velocity for very low frequency systems. The pseudoacceleration A differs very little from the maximum absolute acceleration for systems with a moderate amount of damping for

the whole range of frequencies. This difference reduces with a reduction in the amount of damping.

Oscillators having various different natural periods may in turn be subjected to the same earthquake and their maximum values of acceleration, pseudovelocity and displacement computed. This having been done, the calculated values may then be plotted on the vertical axis of a graph against the corresponding values of natural period or frequency on the horizontal axis. The points thus plotted may be connected to form a curve which is known as a response spectrum. A schematic velocity response spectrum is shown in figure

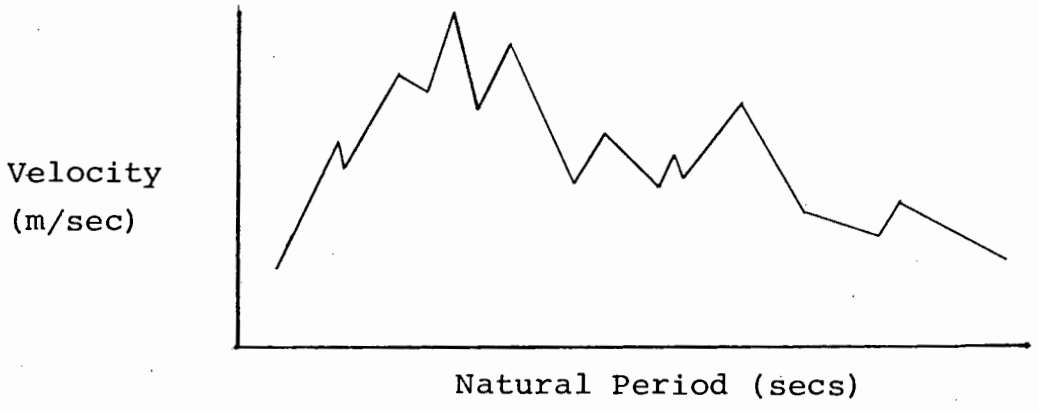

Fig. 6.2 Velocity Response Spectrum

Although the writer prefers to plot Natural Period on the horizontal axis, the authors of some of the references prefer frequency. As a result, both systems appear and both are equally correct.

When subjected to the accelerogram of some other earthquake, each of the oscillators in the set will undergo an entirely different history of movements and will attain maximum values of velocity, etc., which are different from those calculated for the first earthquake. When plotted, these maxima will yield an entirely different response spectrum.

A response spectrum is thus a characteristic of a particular earthquake and is a very useful way of describing the earthquake concerned. Although the computational effort required

to produce a response spectrum is considerable, it needs to be done only once and the possession of it permits a tremendous saving of effort in analysing the earthquake response of structures.

The response spectra for displacement, velocity and acceleration for the N-S component of the earthquake experienced at El Centro in 1940 are plotted on 3 different axes on the same diagram in figure 6.3(a). This is known as a tripartite plot.

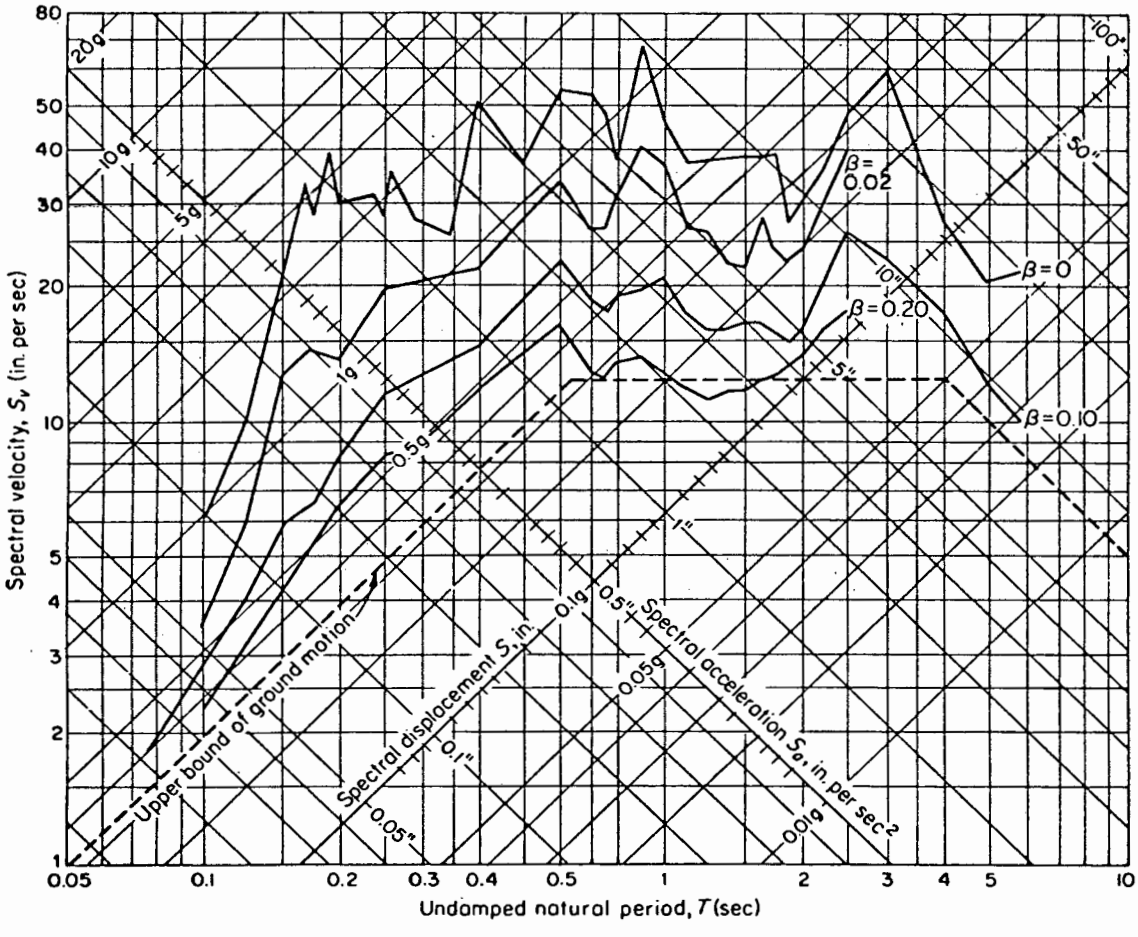

FIGURE 6.3(a) : ELASTIC RESPONSE SPECTRA 1940 EL CENTRO, N-S, EARTHQUAKE

In a single degree of freedom structure for which the natural period of oscillation has been calculated, its response to a particular earthquake may be determined by reading off the appropriate values of maximum acceleration, pseudovelocity or displacement against the known period.

In a multi degree of freedom structure each of the modes may be considered separately. Knowing the natural period for each mode, the corresponding response spectrum ordinate may be read off, thus giving the maximum values of acceleration or velocity or displacement experienced in that mode.

The probability of the maximum values for every mode being reached simultaneously is quite remote. It is common practice to combine the maxima by the Root Mean Square procedure. For example, the combined velocity resulting from maximum velocities v_1, v_2 .....v_n in modes 1 to n is

$$v = \sqrt{v_1^2 + v_2^2 + \ldots\ldots\ldots + v_{n-1}^2 + v_n^2} \qquad (6.4)$$

The calculation of the mode shape and period of oscillation which is required in order to be able to use a response spectrum is simple for a single degree of freedom system and can be performed manually. However, for multi degree of freedom systems the computational effort can become very great and requires the use of a computer.

6.3 Design Spectrum

The earthquake which occurred at El Centro in 1940 is one example of a major earthquake whose motion has been recorded. The response spectrum for this earthquake is shown in figure 6.3(a). In designing a structure to resist earthquake loading using a response spectrum approach, it is necessary to decide what response spectra to use.

It would not be logical to use the El Centro record or any other particular record for the following reasons. Firstly, the recorded ground motion varies considerably from one earthquake to another; indeed, earthquakes occurring at the same site on different occasions would not be expected to exhibit the same ground motion. Secondly, the random nature of the ground shaking results in a response spectrum which is not a smooth curve but has jagged dips and peaks. Using such a curve for design purposes could be misleading for there is every possibility that when in service the structure may be subjected to an earthquake whose response spectrum contains peak values at frequencies for which the response spectrum used in the design had shown dips. Thirdly, the value of displacement, pseudovelocity and acceleration in a response spectrum are maximum values which are instantaneous and may not be approached again during the earthquake. In the short period range ($T<0,5$ sec) such maxima can be the result of single large acceleration pulses in the ground motion. Where these pulses are narrow, they are not expected to be very damaging to structures. In such circumstances, there is some justification for designing to values lower than the peaks in a response spectrum.

This has led to the concept of a design spectrum which represents the average of a number of response spectra within a broad class. A design spectrum plots to a smooth curve and can be regarded as a performance requirement for the structure being designed unlike a response spectrum which is a characteristic of a particular earthquake.

A procedure for establishing a suitable design spectrum for a particular site has been described by Newmark[4] and is described as follows:

Figure 6.3(b) shows a tripartite plot of the El Centro response spectrum plotted against frequency in the form of amplifications of the response relative to the ground motion values of displacement, velocity and acceleration.

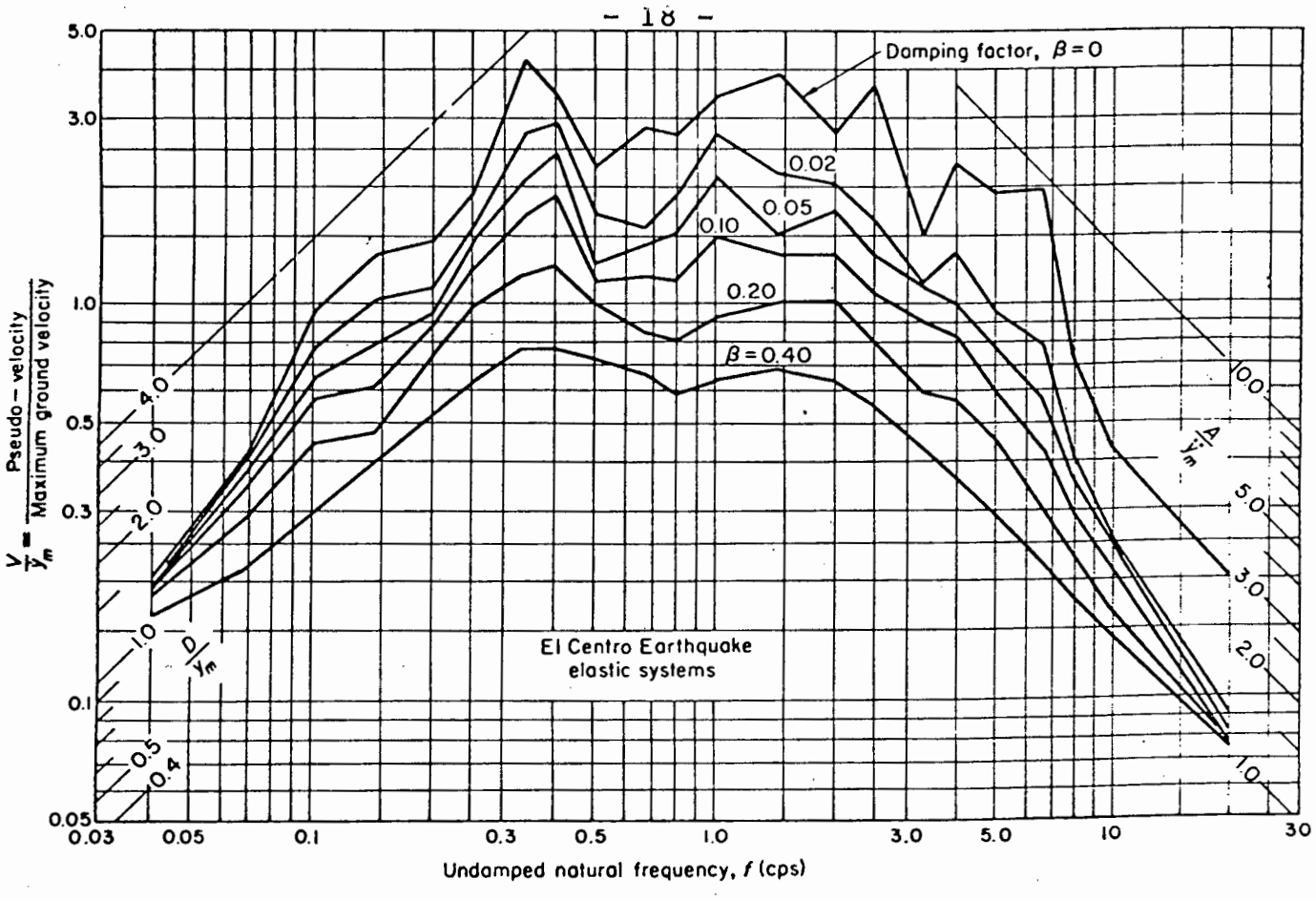

FIGURE 6.3 : DEFORMATION SPECTRA FOR ELASTIC SYSTEMS
(b) SUBJECTED TO THE EL CENTRO EARTHQUAKE

According to Newmark[4], this spectrum is typical of response spectra for nearly all types of ground motion. In the lower frequency systems the responses for all degrees of damping approach the value of the maximum ground displacement. This corresponds to a situation in which a heavy mass is linked to the ground motion by a low stiffness spring. When the ground motion is rapid, the mass does not have time to respond and tends to remain stationary with the result that the displacement of the spring is equal to that of the ground.

In the high frequency range, the acceleration of the mass for all degrees of damping approaches the ground acceleration. This corresponds to a situation in which a light mass is connected to the ground by a very stiff spring which forces the mass to move in the same way as the ground moves.

For intermediate frequency systems, there is an amplification of motion the factor being greatest for acceleration, less for velocity and least for displacement. The greater the

amount of damping, the lower is the amplification factor.

The general nature of response spectra is shown in figure 6.4.

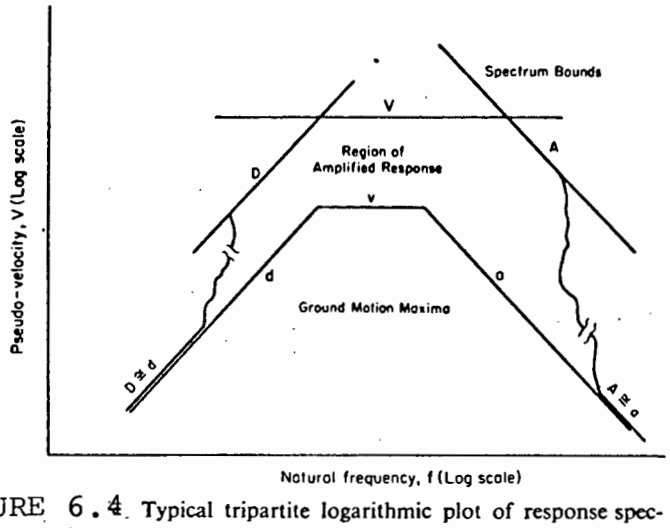

FIGURE 6.4 Typical tripartite logarithmic plot of response spectrum bounds compared with maximum ground motions.

There is a central region of amplified response in which the amplification factors depend on the amount of damping.
In order to illustrate this amplification consider a structure with a natural period of 0,2 secs. and a damping ratio of 0,02. From figure 6.3(a) we read off the maximum acceleration which would be induced in it by the El Centro earthquake. The value is 1,2g. Since the maximum ground acceleration was only 0,33g the amplification of acceleration is $\frac{1,20}{0,33} = 3,64$ times.
Newmark has recommended values of amplification for displacement, velocity and acceleration appropriate to various damping ratios and these are given in table 6.1.

The design spectrum to be used is developed in the following way. Firstly, a spectrum consisting of three straight lines is drawn with the lines representing the maximum values of ground displacement, velocity and acceleration. These values are selected to suit the particular site making the maximum use of available seismic records for the region and supplementing these with judgement where necessary. Secondly, the damping ratio for the structure being designed is estimated.

Some typical values of damping ratios, given by Newmark/ Rosenblueth[5] are produced in table 7.1.

On the basis of the damping ratio adopted, the appropriate amplification factors are taken from table 6.1 and applied to the spectrum representing the ground motion thus leading to the design spectrum to be used in the design. For frequencies above 6 cycles/second, the amplification of acceleration reduces with increasing frequency until a value of 1,0 is reached. This can be seen in figure 6.5.

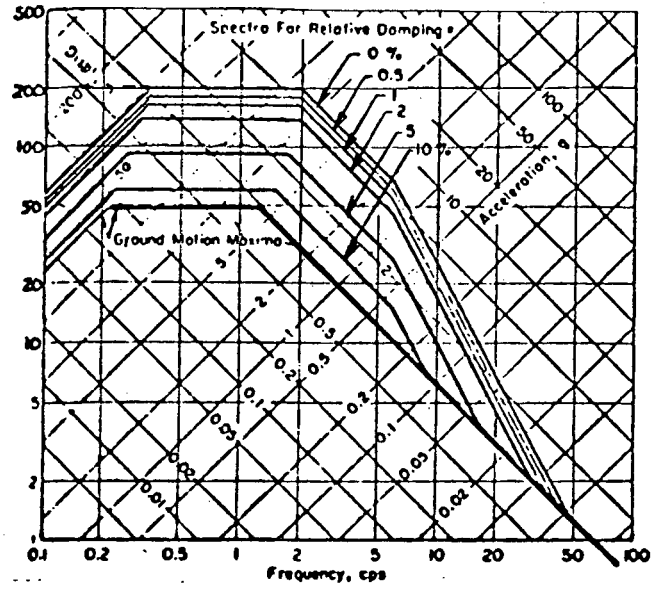

FIGURE 6.5 : BASIC DESIGN SPECTRA NORMALIZED TO 1,0g ELASTIC SYSTEM

This design spectrum may be used to determine the maximum values of acceleration and/or displacement which will be experienced by the structure under the "design earthquake" by the procedure described in 6.2.

TABLE 6.1 : DESIGN SPECTRUM AMPLIFICATION FACTORS

(Newmark, 1972)

DAMPING RATIO (%)	AMPLIFICATION FACTOR FOR		
	Displacement	Velocity	Acceleration
0	2,5	4,0	6,4
0,5	2,2	3,6	5,8
1	2,0	3,2	5,2
2	1,8	2,8	4,3
5	1,4	1,9	2,6
7	1,2	1,5	1,9
10	1,1	1,3	1,5
20	1,0	1,1	1,2

6.4 Equivalent Static Load

The displacements applied to the foundations of structures during earthquakes have components in the horizontal and vertical planes and in typical seismically active areas such as San Francisco the associated accelerations can be expected to attain maximum values of the order of 0,3g. In relation to the gravitational dead and live load for which structures are designed, this would represent a relatively small increase in the vertical loading. However, for most structures a lateral acceleration of 0,3g would induce inertia forces which would be large in relation to other horizontal forces. Consequently, the main emphasis of design using equivalent static loads is directed to horizontal loading.

Certain codes treat this subject simply by specifying a horizontal load applied to each element of the structure equal to a coefficient C times the element mass. This approach is over-simplified since it takes no account of the fact that different structural systems will react differently to a given earthquake depending on their stiffness characteristics.

Improvements to this concept have been incorporated in certain codes for designing buildings to resist earthquakes. The 1957 Los Angeles Building Code gives a formula which results in different values of C for different storeys in the building. The higher values of C relate to the upper floors where the displacements are highest in the lowest mode of oscillation.

The 1959 SEAOC (Structural Engineers Association of California) code is more closely related to dynamic methods since it obtains the seismic coefficient C from the formula $C = \frac{0,05}{\sqrt[3]{T}}$ where T = fundamental period of vibration of the structure. The SEAOC code also takes account of the ductility of the structure in determining the earthquake design loading for a given structure.

The 1965 New Zealand code and the 1970 Uniform Building Code of the U.S.A. are similar in general approach to the SEAOC code. They both include factors appropriate for the seismicity of particular regions in their respective countries.

6.5 Improvement to Accuracy of Manual Calculation by Rayleigh's Principle

In the single degree of freedom system shown in figure 5.3 the mass of the piers was ignored. This is obviously incorrect and we seek a means of taking account of the pier's motion expressed in terms of the top displacement.

A procedure developed by Rayleigh is useful for this purpose. This procedure is based on the fact that the maximum kinetic energy of a freely vibrating system is equal to the maximum potential energy of strain[6]. The procedure involves first assuming the deflected shape during vibration and thence deriving expressions for the kinetic energy and potential strain energy which, when equated lead to the frequency of vibration. The great value of this procedure lies in the fact that any reasonable approximation of the deflected shape will lead to a good approximation of the frequency of vibration.

The application of Rayleigh's procedure is described as follows:

During vibration the kinetic energy of an oscillating mass reaches a maximum when the velocity = 0 and diminishes until it reaches 0 when the displacement (v) reaches a maximum. All the Kinetic Energy (KE) is converted into Potential Strain (PE) as v varies from 0 to max. Equating Kinetic energy and Potential energy, KE = PE

i.e. $\frac{1}{2} M \dot{v}_{max}^2 = \frac{1}{2} K v_{max}^2$ (6.5)

Assuming we have Simple Harmonic Motion (SHM), then from eqn. (5.14)

$v = v_{max} \cos \omega t$

$\therefore \dot{v} = - v_{max} \sin \omega t$ (6.6)

When $t = \frac{\pi}{2}$ $\sin \omega t = 1$ and $\dot{v} = \dot{v}_{max}$ (6.7)

Susbstituting in eqn. (6.5),

$$\tfrac{1}{2} M (-\omega v_{max})^2 = \tfrac{1}{2} K v_{max}^2$$

$$\therefore M\omega^2 = K$$

$$\text{or } \omega^2 = \frac{K}{M} \qquad (6.8)$$

This is in agreement with equation (5.8) and shows that the frequency of vibration of a system moving with SHM can be obtained by considering the energy of the system.

In a complex system containing a number of different elements with masses M_1, M_2 ------ M_n vibrating in the fundamental mode with displacements V_1, V_2 ..... V_n and velocities $\dot{V}_1$, $\dot{V}_2$ ..... $\dot{V}_n$ the energy equation can be written:

$$KE = PE$$

$$\therefore \tfrac{1}{2}(M_1\dot{V}_1^2 + M_2\dot{V}_2^2 + ... + M_n\dot{V}_n^2) = \tfrac{1}{2}(K_1V_1^2 + K_2V_2^2 + ... K_nV_n^2) \qquad (6.9)$$

Expressing the assumed displacement of each element in terms of some known displacement V_a,

$$V_1 = C_1 V_a \qquad \dot{V}_1 = C_1\dot{V}_a$$

$$V_2 = C_2V_a \qquad \dot{V}_2 = C_2\dot{V}_a$$

$$V_n = C_nV_a \qquad \dot{V}_n = C_n\dot{V}_a$$

Substituting in eqn. (6.9):

$$\tfrac{1}{2}(M_1C_1^2\dot{V}_a^2 + M_2C_2^2\dot{V}_a^2 + ... + M_nC_n^2\dot{V}_a^2) = \tfrac{1}{2}(K_1C_1^2V_a^2 + K_2C_2^2V_a^2 + ... K_nC_n^2V_a^2)$$

$$\tfrac{1}{2}\dot{V}_a^2(M_1C_1^2 + M_2C_2^2 + ... M_nC_n^2) = \tfrac{1}{2}(K_1C_1^2 + K_2C_2^2 + ... + K_nC_n^2)V_a^2 \qquad (6.10)$$

If we put $M = (M_1C_1^2 + M_2C_2^2 + ... M_nC_n^2)$

and $K = (K_1C_1^2 + K_2C_2^2 + ... K_nC_n^2)$

$$\text{then } \tfrac{1}{2}V_a^2M = \tfrac{1}{2}KV_a^2 \qquad (6.11)$$

Consequently, the system will vibrate with the same frequency as a simple system with mass M and stiffness K. Expressing the frequency in terms of the deflected shape,

$$\omega = \sqrt{\frac{K}{M}}$$

$$= \sqrt{\frac{K_1C_1^2 + K_2C_2^2 + \ldots. K_nC_n^2}{M_1C_1^2 + M_2C_2^2 + \ldots. M_nC_n^2}} \qquad (6.12)$$

Alternatively an expression for the period may be preferred and this can be written as:

$$T = 2\pi\sqrt{\frac{M_1C_1^2 + M_2C_2^2 + \ldots. + M_nC_n^2}{K_1C_1^2 + K_2C_2^2 + \ldots. + K_nC_n}} \qquad (6.13)$$

Thus, with an assumed deflected shape of the system during vibration we can compute the frequency or period of vibration.

Applying this principle to a pier in the form of a vertical cantilever:

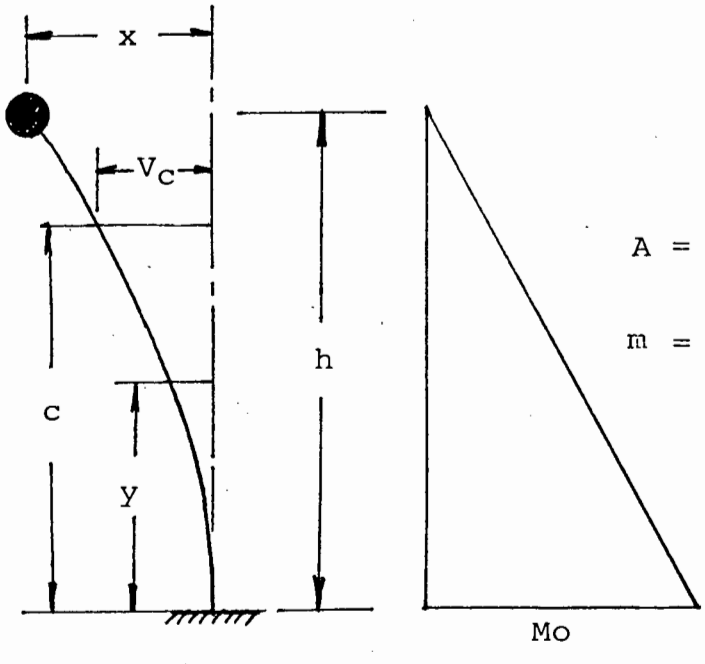

A = concentrated mass at top of pier.

m = mass of pier per metre length.

FIGURE 6.7 : PIER HAVING DISTRIBUTED MASS AND CONCENTRATED MASS

Assume that a reasonable approximation of the deflected shape is that of a massless pier in which V_c is the displacement at some distance C from fixed end. Then

$$V_c = \int_o^c \frac{\left(\frac{h-y}{h}\right) M_o (c-y)\,dy}{EI}$$

$$= \frac{M_o}{EI\ h}\int_o^c (h-y)(c-y)\,dy$$

$$= \frac{M_o}{EI\ h}\left[hcy - (h+c)\frac{y^2}{2} + \frac{y^3}{3}\right]_o^c$$

$$= \frac{M_o c^2}{6EI}\left[3 - \frac{c}{h}\right] \qquad (6.14)$$

The maximum displacement V max, at the end of the pier is given by putting C=h in eqn. (6.14) :

$$V\ max = \frac{M_o h^2}{3EI} \qquad (6.15)$$

In order to express V_c in terms of V_{max}, from eqns. (6.14) and (6.15) :-

$$\frac{V_c}{V_{max}} = \frac{M_o c^2}{6EI}\left(3 - \frac{c}{h}\right) \cdot \frac{3EI}{M_o h^2}$$

$$\therefore V_c = \frac{c^2}{2h^2}\left(3 - \frac{c}{h}\right) V_{max} \qquad (6.16)$$

Differentiating eqn. (6.16) to obtain the velocity;

$$\dot{V}_c = \frac{c^2}{2h^2}\left(3 - \frac{c}{h}\right) \dot{V}_{max} \qquad (6.17)$$

Kinetic energy of element dc $= \frac{1}{2}$ m.dc.$\dot{V}_{max}^2$

$$= \frac{1}{2}\ m.dc\ \frac{c^4}{4h^4}\left(3 - \frac{c}{h}\right)^2 \dot{V}_{max}^2 \qquad (6.18)$$

where m = mass per unit length of pier.

$$\text{K.E. of whole pier} = \int_0^h \tfrac{1}{2}\, m.dc.\, \frac{c^4}{4h^4}\,(3 - \frac{c}{h})^2 \dot{V}_{max}^2$$

$$= \frac{m\dot{V}_{max}^2}{8h^4} \int_0^h (9c^4 - \frac{6c^5}{h} + \frac{c^6}{h^2})\, dc$$

$$= \frac{m\dot{V}_{max}^2}{8h^4} \left[\frac{9c^5}{5} - \frac{6c^6}{6h} + \frac{c^7}{7h^2} \right]_0^h$$

$$= \frac{m\dot{V}_{max}^2}{8h^4}\, h^5 \left[\frac{9}{5} - 1 + \frac{1}{7} \right]$$

$$= \frac{m\dot{V}_{max}^2 h}{8} \left[\frac{63 - 35 + 5}{35} \right]$$

$$= \frac{33}{280}\, m\dot{V}_{max}^2 h \qquad (6.19)$$

$$\text{The K.E. of the lumped mass} = \tfrac{1}{2}\, A\, \dot{V}_{max}^2 \qquad (6.20)$$

where A = concentrated mass at the top of the pier

$$\text{Total K.E.} = \frac{33}{280}\, m\dot{V}_{max}^2 h + A\dot{V}_{max}^2$$

$$= \frac{1}{2} \left\{ A + \frac{33}{140}\, mh \right\} V_{max}^2$$

Thus the system oscillates as though a total mass of $(A + \frac{33}{140}\, mh)$ were concentrated at the top of the pier. In this way we can allow for the participation of the pier mass in the equations of motion by adding a lumped mass of $\frac{33}{140}$ x total mass of the pier to the pier top. This factor is valid for a pier of constant cross section but an expression for an equivalent lumped mass could be derived in the same way for a pier of varying cross section (e.g. tapered pier).

CHAPTER 7

DAMPING

The following is a brief explanation of the effects of damping.

With reference to eqn. 5.6 in chapter 5, the damping constant C multiplied by the velocity gives the damping force. As described by Newmark/Rosenblueth[5], chapter 1.2 there is a particular value of damping constant called "critical damping" denoted by C_{cr}.

$$C_{cr} = 2\sqrt{KM}$$

where K = stiffness and M = mass

Under conditions where $C > C_{cr}$ the system does not oscillate when it is given a displacement or velocity and allowed to move freely, but creeps back, tending to its undeformed state, which it attains after an infinitely long time. When $C < C_{cr}$ the system oscillates but the amplitude decreases with time, tending to its undeformed state.

The ratio $\frac{C}{C_{cr}}$ is defined as the "Coefficient of damping" or "damping ratio".

The effects of damping are illustrated by referring to figure 6.3a. Consider three single-degree-of-freedom structures with periods 0,2 second, 1,0 second and 3,0 seconds. The accelerations experienced by the structures depend upon their damping coefficients and the following values are read off the appropriate curves.

Damping Coefficient	Max. Acceleration		
	T = 0,2 sec	T = 1,0 sec	T = 3,0 sec
0	2,50g	0,80g	0,33g
0,02	1,20g	0,60g	0,25g
0,01	0,70g	0,35g	0,12g
0,20	0,55g	0,20g	0,10g

Figure 6.3a shows how, in the period range between about 0,1 sec and 3,0 sec, the maximum accelerations increase as the damping decreases.

Some typical examples of damping coefficients are given by Newmark/Rosenblueth[5] are reproduced in table 7.1.

TABLE 7.1 : TYPICAL VALUES OF DAMPING

	Stress level	Type and condition of structure	Percentage of critical damping
1.	Low, well below proportional limit, stresses below 1/4 yield point	Vital piping steel, reinforced or prestressed concrete, wood; no cracking;	0,5
		no joint slip	0,5-1,0
2.	Working stress, no more than ½ yield point	Vital piping welded steel, prestressed concrete, well reinforced concrete,	0,5-1,0
		(only slight cracking) reinforced concrete with considerable cracking	2 3 - 5
		Bolted and/or riveted steel, wood structures with nailed or bolted joints	5 - 7
3.	At or just below yield point	Vital piping	2
		Welded steel, prestressed concrete, (without complete loss in prestress)	5
		Reinforced concrete and prestressed concrete	7 - 10
		Bolted and/or riveted steel, wood structures with bolted joints	10 - 15
		Wood structures with nailed joints	15-20
4.	Beyond yield point, with permanent strain greater than yield point limit strain	Piping	5
		Welded steel	7 - 10
		Reinforced concrete and prestressed concrete	10 - 15
		Bolted and/or riveted steel and wood structures	20
5.	All ranges; rocking of entire structure*	On rock, $v_s > 1800$ m/sec	2 - 5
		On firm soil, $v_s \geq 600$m/sec	5 - 7
		On soft soil, $v_s < 600$m/sec	7 - 10

* Higher damping ratios for lower values of shear-wave velocity v_s.

CHAPTER 8

DESCRIPTION AND DEFINITION OF MATHEMATICAL MODEL

The mathematical model represents a bridge designed to carry a 4-lane freeway across a gently dished river valley. A plan, longitudinal section and cross section of the bridge are given in appendix 1. It will be seen that the bridge deck has an overall length of 600 m comprising 8 main spans of 63 m each and two end spans of 48 m each. The deck is supported on vertical piers rising from the valley floor, the height of the longest pier being 75 m. The deck consists of a continuous prestressed concrete hollow box girder with cantilever slabs and the piers are reinforced concrete hollow columns founded on pile caps and spread footings. The possible types of connection between deck and supports are:-

(i) Integral connection

(ii) Sliding bearings

(iii) Pinned bearings

Various combinations of these 3 types are possible and will be discussed in a later chapter.

The mathematical model differs slightly from the real structure in order to simplify the computer input and to facilitate the assimilation of the output. The most notable simplification is the assumption that the deck is level. The deck and pier configuration is given in figure 8.1. For the purposes of this study the deck and piers are assumed to have the properties given in table 8.1.

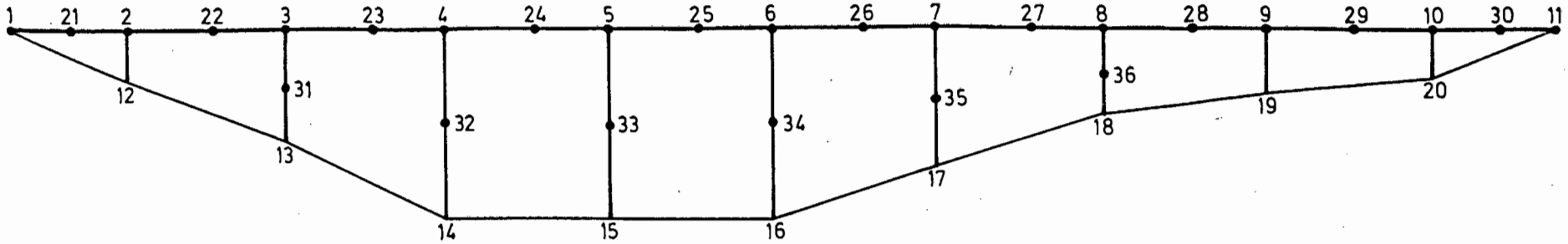

(a) NODE NUMBERS

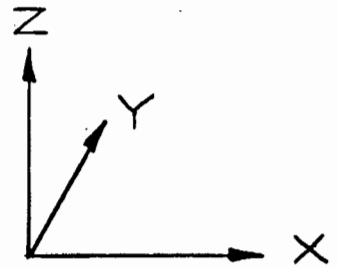

Reference Axis system

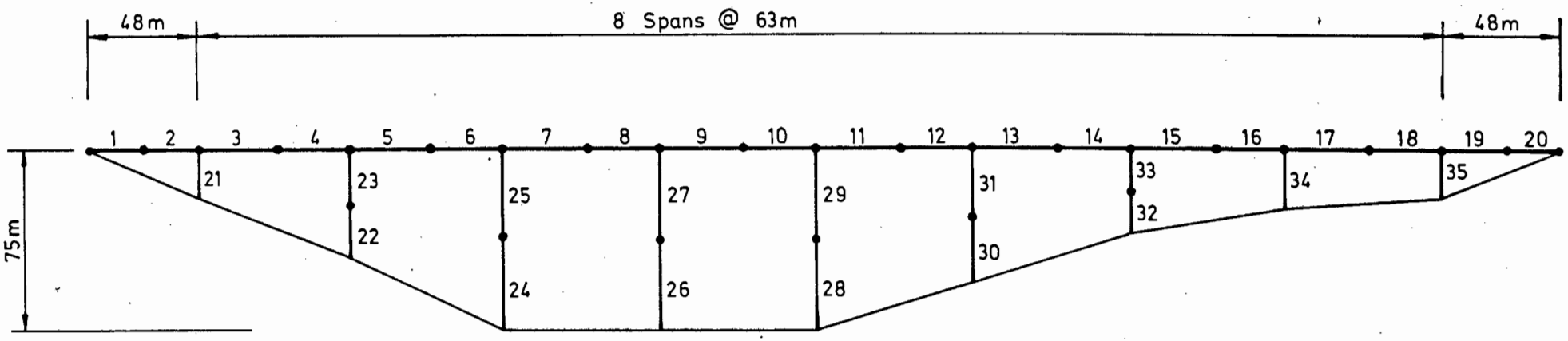

(b) MEMBER NUMBERS AND DIMENSIONS

FIGURE 8.1 : CONFIGURATION OF DECK AND PIERS IN MATHEMATICAL MODEL

Table 8.1 : Properties of the Mathematical Model

Property	Deck	Pier	Units
Modulus of elasticity (E)	30×10^6	30×10^6	kN/m^2
Poisson's Ratio	0,2	0,2	-
Mass Density	2,5	2,5	$tonne/m^3$
Weight Density	24,5	24,5	kN/m^3
Axial Area	10,40	9,44	m^2
Shear Area (longitudinal)	4,0	4,8	m^2
Shear Area (lateral)	6,4	5,6	m^2
Torsional Inertia (J)	56,7	47,5	m^4
Moment of Inertia, Iyy	156,4	50,8	m^4
Moment of Inertia, Ixx	21,7	21,5	m^4

The coordinates of the main node points are given in table 8.2:

Table 8.2 : Coordinates of Node Points

NODE NO.	COORDINATES	
	X	Z
1	0	0
2	48	0
3	111	0
4	174	0
5	237	0
6	300	0
7	363	0
8	426	0
9	489	0
10	552	0
11	600	0
12	48	-20
13	111	-45
14	174	-75
15	237	-75
16	300	-75
17	363	-55
18	426	-35
19	489	-25
20	552	-20

CHAPTER 9

RESPONSE SPECTRUM ANALYSIS OF THE MODEL

9.1 General

The following examples illustrate the method described in chapter 6.2 for determining the displacements and forces in the structure resulting from a given ground motion. In each case it is necessary to calculate the mass and the stiffness of the structure when moving in a particular mode. This leads to the period of that mode. Finally, the values of displacement, velocity or acceleration for the calculated period may be read off the chosen response spectrum using an appropriate damping ratio. The forces acting on the structure may be deduced either from the acceleration or from the displacement.

The spectrum used may be either a response spectrum of a particular earthquake or an idealised design spectrum. The former will indicate how the structure would have responded to the particular earthquake whilst the latter will produce responses to a hypothetical ground motion. Either type of spectrum will serve to illustrate the analysis of the structural responses but for design purposes it would be preferable to use the design spectrum.

All the computational work in this thesis has been based on the response spectrum of the 1940 El Centro earthquake. In retrospect it is now realised that it would have been preferable to set up a suitable design spectrum along the lines described in 6.3. However, the emphasis of this thesis is qualitative rather than quantitative and the response spectrum which has been used serves the purpose of illustrating the techniques equally well.

In order to minimise any misleading comparisons in the calculations resulting from the peaks and dips of the jagged

shaped response spectrum an unusually high damping ratio of 0,20 was assumed as the jaggedness is less pronounced with higher damping ratios. The calculations must therefore be regarded as an academic exercise showing how the mathematical model would have responded to the 1940 El Centro earthquake if the structure had possessed a damping ratio of 0,20.

In reality the real bridge would have a much lower damping ratio. If it is assumed that our structure consists of reinforced and prestressed concrete and that, under earthquake loading, it is undergoing stresses just below yield point, then from table 7.1 an appropriate damping coefficient would be in the range of 7% to 10%.

The following calculation illustrates the setting up of a suitable design spectrum which can be compared with the response spectrum which was used.

In assuming values of displacement, velocity and acceleration for the ground motion, reference is made to the values recorded in the 1940 El Centro earthquake. These values have been scaled down by a factor of 0,7 so as to represent an earthquake with a maximum ground acceleration of approx. 0,2g.

	Displacement	Velocity	Accn.
1940 El Centro values	0,210 m	0,35 m/s	0,32g
0,7 x El Centro values	0,147 m	0,25 m/s	0,22g
Amplification factor from table 6.1 for damping ratio of 7%	1,2	1,5	1,9
Design spectrum value	0,176 m	0,38 m/s	0,43g

The values for the ground motion as well as the design spectrum have been superimposed on fig. 9.2 and it will be seen that the design spectrum values do not differ greatly from those of the 20% damping ratio values of the El Centro response spectrum used in the computations.

9.2 Worked Examples assuming piers massless

9.2.1 Example 1

Consider a mode of oscillation of the model in which the displacement of the deck takes place along its own axis. Assuming the deck to be supported by pinned supports at every pier and sliding supports at both abutments and ignoring the mass of the piers, the stiffness applicable to this motion is obtained as follows:-

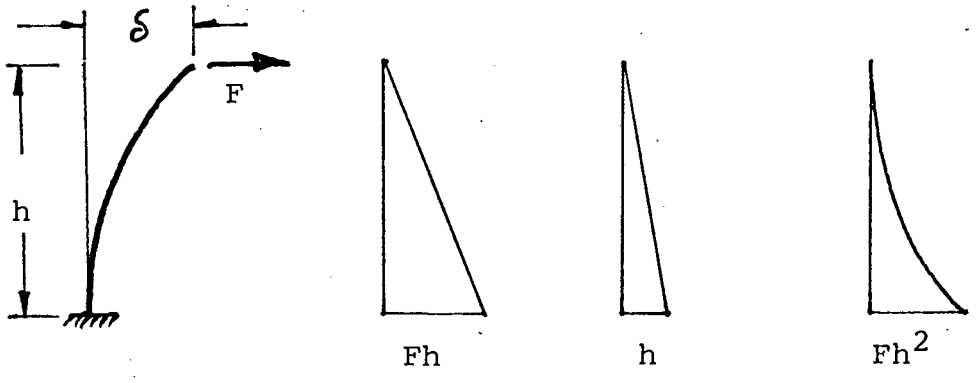

FIGURE 9.1 : STIFFNESS OF VERTICAL CANTILEVER

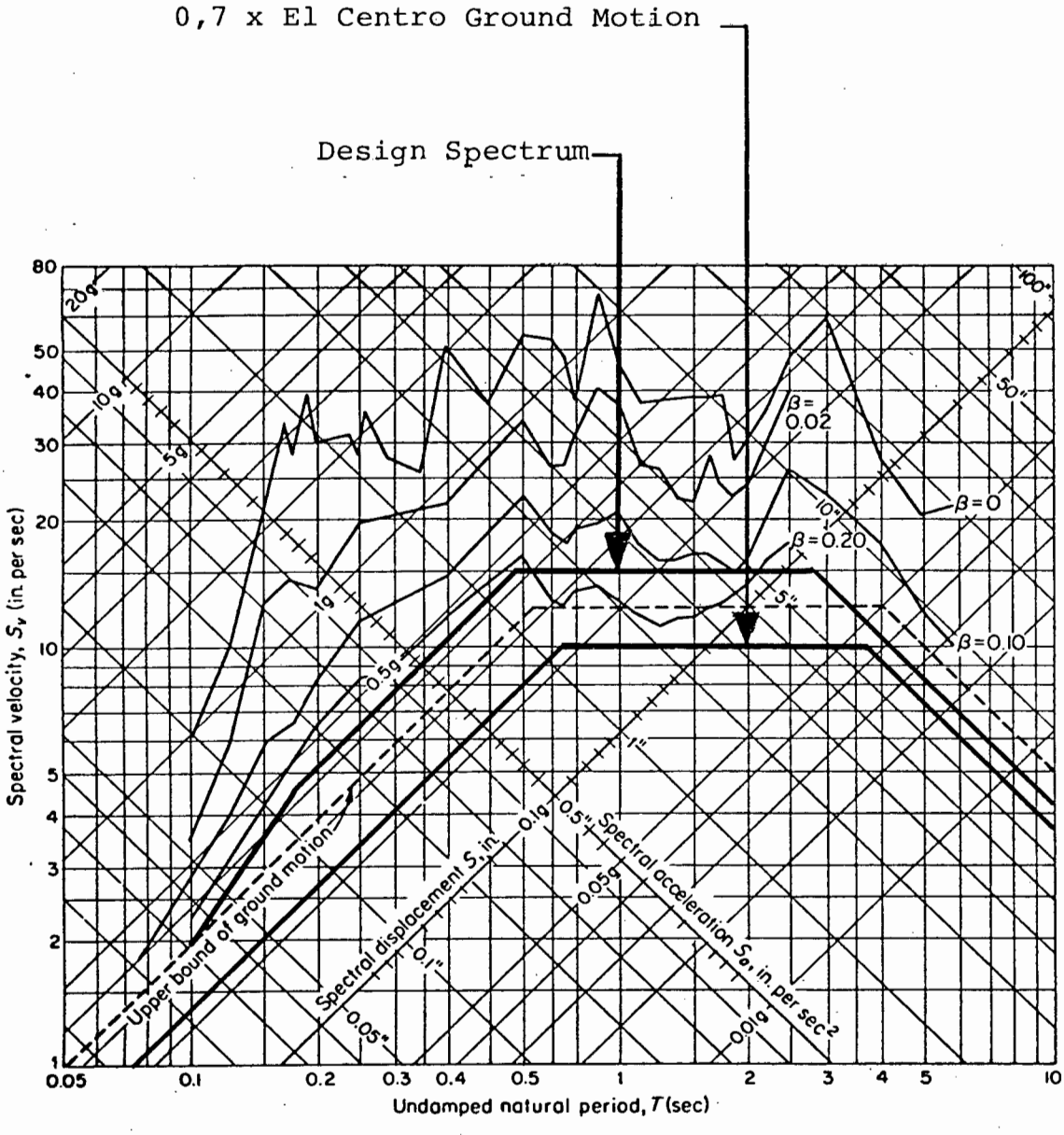

FIGURE 9.2 : ELASTIC RESPONSE SPECTRA 1940 EL CENTRO, N-S, EARTHQUAKE

$$\delta = \int_0^h \frac{Fh.\ h.\ dh}{EI}$$

$$= \frac{1}{3}\frac{Fh^3}{EI}$$

$$\therefore \frac{F}{\delta} = \frac{3EI}{h^3} = \text{Stiffness K}$$

The displacement of the deck along its axis displaces all the pier tops horizontally by the same amount and can be expressed by a single dimension. It therefore behaves as a single-degree-of-freedom structure in this mode.

Total stiffness $K = K_1 + K_2 + \ldots\ldots K_9$

$$\text{i.e. } K = 3EI\ (\frac{1}{h^3} + \frac{1}{h_3^3} + \ldots\ldots \frac{1}{h_9^3} + \frac{1}{h_{10}^3})$$

From table 8.1: $E = 30 \times 10^6\ kN/m^2$

$$I = 21,5\ m^4$$

Table 9.1 : Pier Stiffness

Pier Nodes	h	$\frac{1}{h^3}$	K
12-2	20	$125,0 \times 10^{-6}$	241 875
13-3	45	11,0 "	21 285
14-4	75	2,4 "	4 644
15-5	75	2,4 "	4 644
16-6	75	2,4 "	4 644
17-7	55	6,0 "	11 610
18-8	35	23,3 "	45 086
19-9	25	64,0 "	123 840
20-10	20	125,0 "	241 875
		$361,5 \times 10^{-6}$	699 503

Thus $K = 3 \times 30 \times 10^6 \times 21,5 \times 361,5 \times 10^{-6}$

$= 699\ 503$ kN/m

M = Cross sectional area of deck x length of deck x mass density

$= 10,4 \times 600 \times 2,5$

$= 15\ 600$ tonnes

In eqn. 19:

$$T = 2\pi \sqrt{\frac{15\ 600}{699\ 503}}$$

$= 0,938$ secs.

i.e. the period of oscillation in this assumed mode is 0,938 sec.

The response spectrum for the 1940 El Centro earthquake is shown in figure 9.2.

Entering the chart with T = 0,938 secs and assuming the damping coefficient $\beta = 0,20$ we read off

max displacement = $\delta = 2,0$ inches = 0,051 m

max acceleration = $a = 0,24g = 2,35$ m/sec^2

Calculation of Forces induced :

(a) by considering displacement x stiffness :

$F = 0,051 \times 699\ 503$

$= \underline{35\ 675\ kN}$ or, as a check :

(b) from acceleration :

F = mass x acceleration

$= 15\ 600 \times 2,35$

$= \underline{36\ 600\ kN}$

Theoretically both values of F should be identical. However, the graphical plot does not permit that degree of accuracy.

If required for design purposes, the force at the top of each individual pier may be obtained by multiplying the displacement by the individual pier stiffness.

In a very few lines of calculation, we have obtained approximate values of the period of oscillation, the displacement and the forces acting on the piers in one mode of vibration.

9.2.2 Example 2

The effect of providing pinned joints at some of the pier tops while permitting sliding at the others can be evaluated in the same way. Consider the case where pier tops 6, 7 and 8 are pinned, assuming, provisionally, that the sliding bearings at the other pier tops are frictionless.

$$K = 3EI \left[\frac{1}{h_6^3} + \frac{1}{h_7^3} + \frac{1}{h_8^3}\right]$$

$$= 3 \times 30 \times 10^6 \times 21{,}5\ (2{,}4 + 6{,}0 + 23{,}3) \times 10^{-6}$$
$$= 61\ 340\ \text{kN/m}$$

$$T = 2\pi \sqrt{\frac{15\ 600}{61\ 340}}$$
$$= 3{,}17\ \text{secs.}$$

Again from figure 9.2 with $\beta = 0{,}20$

Max displacement δ = 9" = 0,229 m
Max acceleration a = 0,095g = 0,932 m/sec^2

Induced force:
(a) from stiffness : $F = K\delta$
$= 61\ 340 \times 0{,}229$
$= 14\ 047$ kN or, as a check:

(b) from acceleration : $F = Ma$

$= 15\ 600 \times 0{,}932$

$= \underline{14\ 539\ kN}$

Considering now the effect of friction on the sliding bearings, the deck load on typical pier = 16 380 kN and the coefficient of friction, μ, for teflon on stainless steel is approximately 0,03 so that the maximum possible horizontal force transmitted through the bearing is $16\ 380 \times 0{,}03 = 491$ kN.

In this example pier tops 6, 7 and 8 were considered pinned. On the assumption that the other pier tops had frictionless bearings ($\mu = 0$) the displacement of the deck was calculated to be 0,229 m. Table 9.2 shows the force 0,229K that would be required for each pier to displace it by 0,229 m where K is the stiffness shown in table 9.1

Table 9.2 : Forces Generated by 0,229 m at Pier Tops

Pier Top at Nodes	0,229K (kN)
2	55 389
3	4 874
4	1 063
5	1 063
6	1 063
7	2 659
8	10 325
9	28 359
10	55 389

It is evident that a displacement of 0,229 m would cause the maximum possible sliding resistance to be exceeded at each of the sliding bearings and that the sum of the frictional forces would be 6 x 491 = 2 946 kN compared with the sum of the force at the pinned bearings of 14 047 kN. Our assumption that the sliding bearings are frictionless is clearly an oversimplification and the limited resistance offered by the sliding bearings will add to the stiffness of the structure and decrease the period T. As a result, the displacements will decrease leading to a reduction in the pinned bearing forces. Although oversimplified, the assumption of frictionless bearings leads to conservative values of bearing forces and displacements to be accommodated.

The inclusion of the sliding forces in the equations of motion is not simple because of the fact that the bearing force is no longer related to the stiffness K once the displacements have exceeded those which would cause the bearing to slide.

In configurations with fewer sliding bearings the relative effect of the sliding forces will become less significant, particularly when some of the shorter stiffer piers have pinned connections to the deck. In example 1, for instance, the forces on the pinned bearings totalled 35 675 kN. With an end reaction at the abutment of 6 240 kN the sliding force at each abutment = 6 240 x 0,03 = 187 kN.

Thus relationship $\frac{\text{sliding forces}}{\text{pinned forces}} = \frac{2 \times 187}{35\ 675}$

$= 1{,}05\%$

For practical purposes it is considered justifiable to ignore the frictional force in the sliding bearings

9.2.3. Example 3

In the case where the deck is connected to the abutment by means of a pinned bearing permitting no sliding in X-direction the stiffness K becomes infinite. Since period $T = 2\pi\sqrt{\frac{M}{K}}$,

when $K = \infty$, $T = 0$. In this situation there is no amplification and the deck moves with the ground. From figure 9.2 the upper bound of ground acceleration = 0,33g. The resulting inertia force applied to the deck via the abutment bearings is given by

$$F = 15\ 600 \times 0{,}33 \times 9{,}81$$
$$= 50\ 502\ kN$$

Even though there is no amplification of the ground acceeration with this arrangement, the inertia force is higher than that of most of the other configurations as can be seen from the results in chapter 14, table 14.1. This is because its period is so much less than the others whose periods bring them into the range where the basic ground acceleration is well below the upper bound of ground acceleration.

9.3 Adjustment to allow for pier mass

Rayleigh's method, as described in chapter 6.5 is now used to adjust the results of the two worked examples in 9.2 to make allowance for the pier mass.

The equivalent lumped masses for the piers are obtained as follows:-

Pier mass per metre = 9,44 x 2,5
= 23,6 tonnes.

TABLE 9.3 : EQUIVALENT LUMPED MASS REPRESENTING PIER MASSES

Pier Nodes	h	Total pier mass (t)	$\frac{33}{140}$ x pier mass (t)
12-2	20	472	111
13-3	45	1062	250
14-4	75	1770	417
15-5	75	1770	417
16-6	75	1770	417
17-7	55	1298	306
18-8	35	826	195
19-9	25	590	139
20-10	20	472	111
			2363

Thus in examples 1 and 2 in chapter 9 the accuracy of the calculations would be greatly improved by the simple technique of adding the equivalent pier mass to the mass of the deck, thus:

deck mass	=	15 600 t
equiv. pier mass	=	2 363 t
Effective total mass M_e	=	17 963 t

The amended periods are obtained as follows:
The previous values for massless piers are shown in brackets for comparison.

Example 1

$$T = 2\pi\sqrt{\frac{17\ 963}{699\ 503}}$$

$= 1{,}007$ secs (0,938)

Example 2

$$T = 2\pi\sqrt{\frac{17\ 963}{61\ 340}}$$

$= 3{,}400$ secs (3,17)

9.4 Integral Connections between deck and piers

Although the above examples have employed pinned connections for ease of calculation, some or all of the connections could equally well have been integral with the piers since the stiffness of the system could still have been expressed in terms of a total axial force in the deck per unit axial displacement.

CHAPTER 10

USE OF COMPUTER FOR RESPONSE SPECTRUM AMALYSIS

In the examples used in chapter 9, we were dealing with a mode of vibration in which the structure acted as a single-degree-of-freedom system and the determination of the mode shape was very simple. As mentioned in chapter 6.2, there will be other modes of vibration and these may be more complex to analyse.

It is usual for the forces and displacements to be dominated by responses in the lower modes (i.e. the modes with the longest periods of vibration). For mode shapes involving longitudinal displacements of the model it is fairly obvious that the mode shape chosen will be the longest period mode and the one which will dominate the forces in that direction. The displacements and forces obtained manually can therefore be used with some confidence as effectively representing the sum of the effects of all modes contributing to longitudinal displacement.

The determination and ranking of modes in the transverse and vertical directions are not so obvious and it is necessary to evaluate the effects of a number of modes in order to ensure that all significant modes have been considered. The number of modes that need to be considered can best be determined by trial and error.

The are a number of computer program packages capable of performing the analysis required. The one selected for use in the computational work of this thesis is the one known as SAP IV[7]. The program is capable of performing a time history analysis (direct step-by-step integration, as described in chapter 6.1) or a response spectrum analysis as described in chapter 6.2. The method used for the work in this thesis is the response spectrum method.

CHAPTER 11

INPUT REQUIRED FOR SAP IV PROGRAM

The input required to run this program includes information regarding the numbers of nodal points, element types, load cases and frequencies required. The information required for the beam elements describes their geometric and material properties as well as the connection conditions at their ends.

The response spectrum information is given in the following form:

(a) Direction factors: Factors by which the excitation must be multiplied for each of the directions X, Y and Z are required. The factors used were 1,0, 1,0 and 0,6 respectively.

(b) A definition of the response spectrum in the form of a list of points on the curve of acceleration (or displacement) plotted against period. The response spectrum used was that of the 1940 El Centro earthquake using the values for 20% damping.

It was read into the computer in the form of a list of values of period in seconds with corresponding values of acceleration, the values chosen being those of the peaks and dips in the response spectrum curve.

CHAPTER 12

OUTPUT FROM SAP IV

The output obtained from SAP IV is as follows:

12.1 A listing of all input data.

12.2 Information regarding dimensions and manipulation of stiffness matrix.

12.3 A list of the periods of the modes computed, arranged in decreasing order.

12.4 A tabulation of the shapes of each mode expressed as sets of relative displacements (translational and rotational) at each node.

12.5 A tabulation of the absolute displacements (translational and rotational) at each node for each mode as well as a root-sum-square combination of the displacements in all the computed modes.

12.6 A listing of the forces and moments at both ends of each element, based on the square root of the sum of the squares of the forces in the individual modes.

CHAPTER 13

PROGRAMME OF PARAMETER CHANGES

The programme of parameter changes was set up taking account of the limitations set in chapter 1 (Aim of Thesis) and chapter 4 (Results Required from Earthquake Analysis).

The broad aim was to test the sensitivity of the structure to excitation in the longitudinal, transverse and vertical directions and to examine the effects of varying the types of connection between piers and deck. In order to fully explore these effects, some configurations at the extremes of the ranges were considered in spite of their being unrealistic in practice. For example, it would be impractical to provide "pinned" connections at the top if every pier since this would result in very large horizontal reactions being set up between the deck and the short, stiff piers near the ends of the deck under the action of temperature, creep and shrinkage.

In this model, bearings are always provided in pairs. In each pair of bearings one is always restrained against transverse (Y) displacement. "Pinned" bearings in the following descriptions refer to pairs in which neither bearing is free to displace in longitudinal (X) direction. "Sliding" bearings refer to pairs in which both bearings are free to displace in X direction. Vertical (Z) displacement is not permitted in any bearing arrangement. Both bearing arrangements permit rotation about Y axis and neither permit rotation about the X axis. Rotation about the Z axis can occur with sliding bearings but not with pinned bearings.

The following are tabulations of the various structural systems analysed using SAP IV. In the tables the symbols have the following meanings:

- : Bearing permitting sliding in X-direction

P : Pinned bearing

F : Fixed (deck monolithic with pier)

Although the output of SAP IV gives the displacements separately for each individual mode, the forces given are simply the RMS value of all the modes considered. Some of the configurations were re-run a number of times considering a different number of modes each time. This was of interest in comparing the forces associated with the lower modes with those associated with the higher modes.

13.1 For Excitation in X-direction

1 (abut)	2	3	4	5	6	7	8	9	10	11 (abut)	No. of Modes considered
-	-	-	P	P	P	P	-	-	-	-	12
-	-	-	-	-	P	P	P	-	-	-	12
-	-	-	-	P	P	P	P	-	-	-	12
-	-	-	-	-	P	P	P	P	-	-	12
-	-	-	-	P	P	P	P	P	-	-	12
-	-	-	P	P	P	P	P	-	-	-	12
-	-	P	P	P	P	P	P	-	-	-	12
-	-	P	P	P	P	P	P	P	-	-	12
-	-	P	P	P	P	P	P	P	P	-	12
-	P	P	P	P	P	P	P	P	P	-	12
-	-	-	-	-	-	P	P	P	-	-	12
-	-	-	-	-	-	F	F	F	-	-	12
-	-	-	F	F	F	F	-	-	-	-	12
-	-	-	-	-	F	F	F	-	-	-	12
-	-	-	-	F	F	F	F	-	-	-	12
-	-	-	F	F	F	F	F	-	-	-	12
-	-	-	-	-	F	F	F	F	-	-	12
-	-	F	F	F	F	F	F	F	-	-	12
-	F	F	F	F	F	F	F	F	F	-	12
-	P	P	P	P	P	P	P	P	P	-	1
-	P	P	P	P	P	P	P	P	P	-	3
-	P	P	P	P	P	P	P	P	P	-	6
-	P	P	P	P	P	P	P	P	P	-	9

13.2 For Excitation in Y-direction

1 (abut)	2	3	4	5	6	7	8	9	10	11 (abut)	No. of Modes considered
-	P	P	P	P	P	P	P	P	P	-	1
-	P	P	P	P	P	P	P	P	P	-	3
-	P	P	P	P	P	P	P	P	P	-	6
-	P	P	P	P	P	P	P	P	P	-	9
-	P	P	P	P	P	P	P	P	P	-	12
-	F	F	F	F	F	F	F	F	F	-	12

13.3 For Excitation in Z-direction

-	P	P	P	P	P	P	P	P	P	-	12

CHAPTER 14

RESULTS OF COMPUTATIONS

The output which is of interest in this study consists of:

a) Maximum displacements of the deck.

b) Horizontal reactions between deck and pier tops.

c) Bending moments at bases of piers.

d) The periods of oscillation.

In each case the relevant output has been extracted from the computer print-out sheets and presented in graphical or tabular form. Each graph or table is prefaced by a description of the results presented.

14.1 Displacement in the various modes

In order to illustrate how the displacements in certain modes predominate in any given direction, the displacements for a particular configuration (i.e. pinned bearings at all pier tops and sliding bearings at abutments) have been extracted from the output and tabulated.

Tables 14.1, 14.2 and 14.3 list the displacements in each of the 12 modes of oscillation as well as the combined displacements expressed as the "root-sum-square" of the displacements in the individual modes. Displacements for the configuration in which all pier tops are pinned to the deck are shown in figure 14.1 for direction X, figure 14.2 for direction Y and figure 14.3 for direction Z.

TABLE 14.1 : X-DISPLACEMENTS FOR CONDITION : BEARINGS AT ALL PIER TOPS PINNED IN X-DIRECTION
BEARINGS AT BOTH ABUTMENTS SLIDING IN X-DIRECTION

MODE NO		1	2	3	4	5	6	7	8	9	10	11	12	Σ_1^{12}
PERIOD (SECS)		2,151	1,245	1,092	0,796	0,581	0,506	0,474	0,471	0,470	0,467	0,463	0,433	
NODE	REMARKS	DISPLACEMENTS mm												
1	Tops of piers	0	0	56	0	0	0	0	0	0	-1	0	0	56
2		0	0	56	0	0	0	0	0	0	-1	0	0	56
3		0	0	59	0	0	0	0	0	0	-1	0	0	59
4		0	0	59	0	0	0	0	0	0	-1	0	0	59
5		0	0	59	0	0	0	0	0	0	-1	0	0	59
6		0	0	59	0	0	0	0	0	0	-1	0	0	59
7		0	0	58	0	0	0	0	0	0	-1	0	0	58
8		0	0	56	0	0	0	0	0	0	-1	0	0	56
9		0	0	54	0	0	0	0	0	0	-1	0	0	54
10		0	0	52	0	0	0	0	0	0	-1	0	0	52
11		0	0	52	0	0	0	0	0	0	-1	0	0	52
31	Mid-height of piers	0	0	19	0	0	0	0	0	0	0	0	0	19
32		0	0	23	0	0	0	0	-2	0	13	0	0	26
33		0	0	23	0	0	0	0	0	-1	14	0	0	27
34		0	0	23	0	0	0	0	2	0	17	0	0	28
35		0	0	19	0	0	0	0	0	0	0	0	0	19
36		0	0	18	0	0	0	0	0	0	0	0	0	18

TABLE 14.2 : Y-DISPLACEMENTS FOR CONDITION : ABUTMENTS AND ALL PIER TOPS PINNED TO DECK IN Y-DIRECTION

MODE NO		1	2	3	4	5	6	7	8	9	10	11	12	Σ_1^{12}
PERIOD (SECS)		2,151	1,245	1,092	0,796	0,581	0,506	0,474	0,471	0,470	0,467	0,463	0,433	
NODE	REMARKS	DISPLACEMENTS mm												
1	Abutment	0	0	0	0	0	0	0	0	0	0	0	0	0
2	Pier	5	0	0	7	-2	0	0	0	0	0	-7	0	11
3	Pier	55	-3	0	30	-6	0	0	0	0	0	-12	0	64
4	Pier	145	-4	0	16	1	0	0	0	0	0	10	0	146
5	Pier	198	-1	0	-24	4	0	0	0	0	0	-2	0	199
6	Pier	171	3	0	-12	-4	0	0	0	0	0	7	0	172
7	Pier	88	4	0	25	-1	0	0	0	0	0	11	0	94
8	Pier	21	2	0	30	7	0	0	0	0	0	-5	0	38
9	Pier	0	0	0	9	5	0	0	0	0	0	-17	0	20
10	Pier	-1	0	0	0	1	0	0	0	0	0	-7	0	7
11	Abutment	0	0	0	0	0	0	0	0	0	0	0	0	0

TABLE 14.3 : Z-DISPLACEMENT FOR CONDITION : BEARINGS AT ALL SUPPORTS PINNED IN Z-DIRECTION

MODE NO		1	2	3	4	5	6	7	8	9	10	11	12	12
PERIOD (SECS)		2,151	1,245	1,092	0,796	0,581	0,506	0,474	0,471	0,470	0,467	0,463	0,433	
NODE	REMARKS	DISPLACEMENTS mm												
1		0	0	0	0	0	0	0	0	0	0	0	0	0
21		0	0	0	0	0	0	-0,14	0	0	0	0	+0,04	0,14
2		0	0	0	0	0	0	0	0	0	0	0	0	0
22		0	0	0	0	0	0	+0,40	0	0	0	0	-0,10	0,41
3		0	0	0	0	0	0	0	0	0	0	0	0	0
23		0	0	0	0	0	0	-0,52	0	0	0	0	+0,08	0,52
4		0	0	0	0	0	0	0	0	0	0	0	0	0
24		0	0	0	0	0	0	+0,43	0	0	0	0	+0,01	0,43
5		0	0	0	0	0	0	0	0	0	0	0	0	0
25		0	0	0	0	0	0	-0,16	0	0	0	0	-0,09	0,18
6		0	0	0	0	0	0	0	0	0	0	0	0	0
26		0	0	0	0	0	0	-0,17	0	0	0	0	+0,09	0,19
7		0	0	0	0	0	0	0	0	0	0	0	0	0
27		0	0	0	0	0	0	+0,43	0	0	0	0	0	0,43
8		0	0	0	0	0	0	0	0	0	0	0	0	0
28		0	0	0	0	0	0	-0,51	0	0	0	0	-0,08	0,51
9		0	0	0	0	0	0	0	0	0	0	0	0	0
29		0	0	0	0	0	0	+0,39	0	0	0	0	+0,10	0,41
10		0	0	0	0	0	0	0	0	0	0	0	0	0
30		0	0	0	0	0	0	-0,13	0	0	0	0	-0,04	0,14
11		0	0	0	0	0	0	0	0	0	0	0	0	0

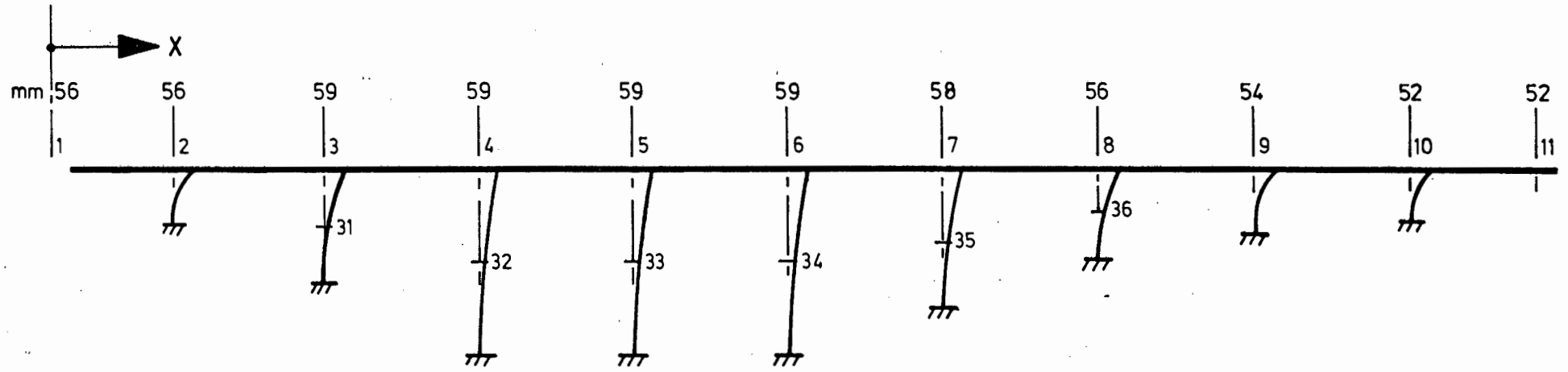

ELEVATION

FIGURE 14.1 : DISPLACEMENTS IN X-DIRECTION (LONGITUDINAL) FOR MODE Nº. 2
DECK PINNED AT ALL PIER TOPS, SLIDING AT ABUTMENTS

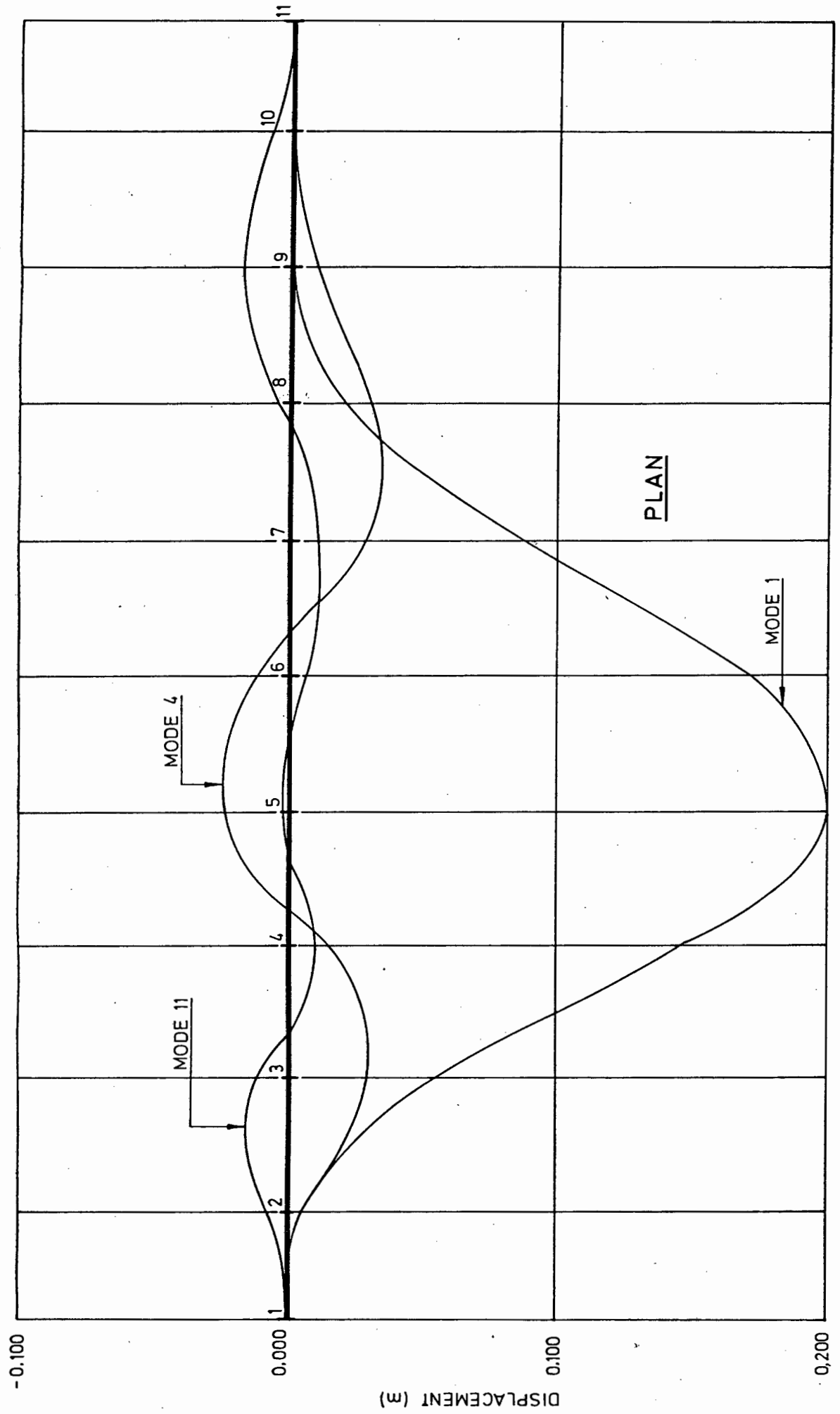

FIGURE 14.2 : DISPLACEMENTS IN Y-DIRECTION (TRANSVERSE)

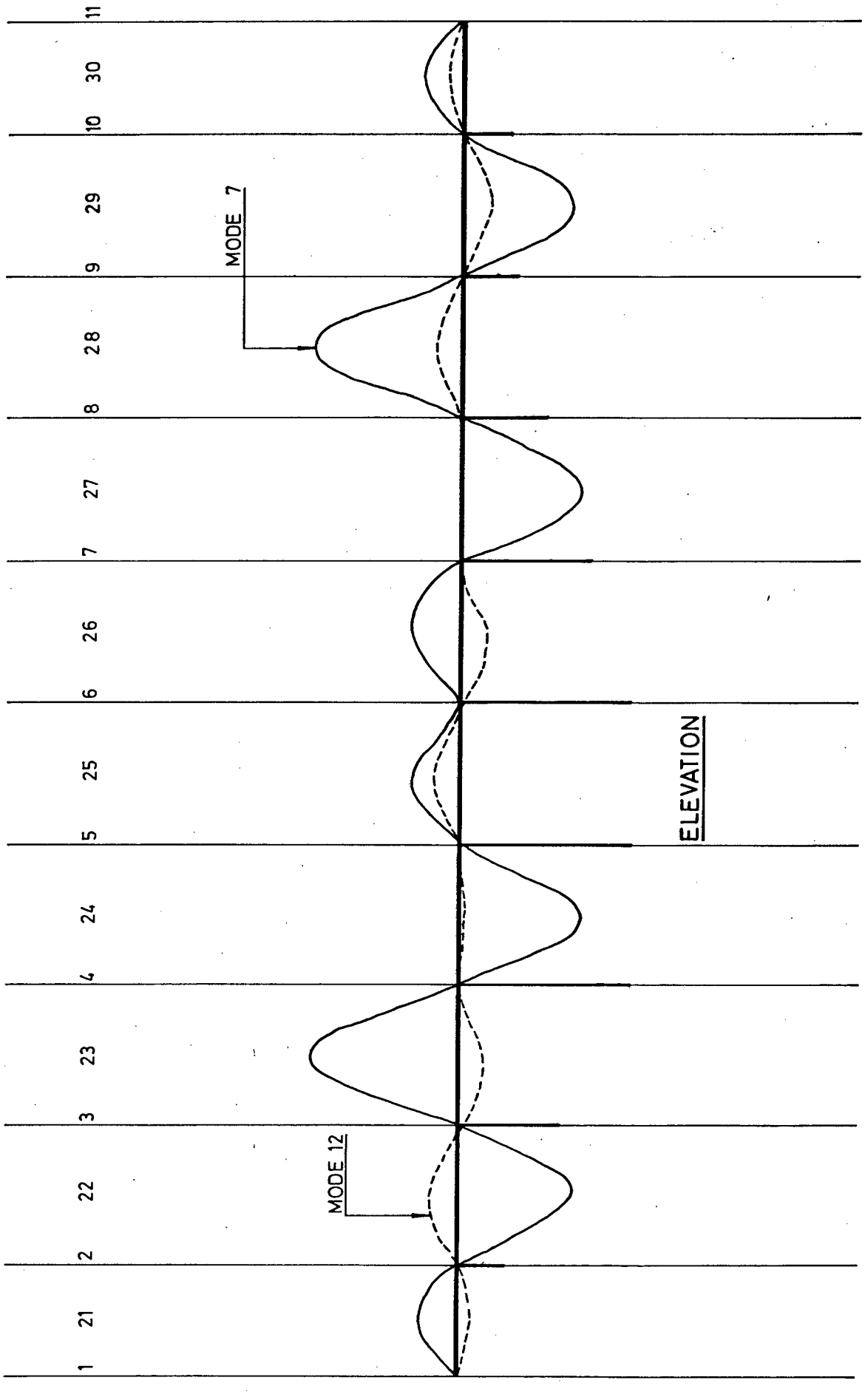

FIGURE 14.3 : DISPLACEMENTS IN Z-DIRECTION (VERTICAL)

14.2 X-Excitation

Table 14.4 lists the computed results for the various configurations of deck to pier connections and gives the following information for each configuration:

i) The type of connection:
P = pinned
F = integral

ii) The maximum displacement.

iii) The number of the mode which is the main contributer to the maximum displacement.

iv) The period of that mode.

v) Horizontal deck-to-pier reaction at each pier. (A blank indicates zero reaction due to a sliding bearing).

iv) The sum of all these reactions.

vii) The maximum individual pier base moment.

14.3 Y-Excitation

14.3.1 Pinned connections between piers and deck

Only one configuration of pinned and sliding connections was computed. At every pier top the connection was released for moment about the Y-axis and the Z-axis (i.e. pinned for longitudinal movements). At each abutment the connection was released for X-translation, Y-rotation and Z-rotation. The forces and moments are given in table 14.5.

TABLE 14.4 : X-EXCITATION : FORCES AND DISPLACEMENTS FOR VARIOUS DECK/PIER CONNECTION CONFIGURATIONS

CONNECTION CONDITION	DISP (mm)	MODE (No)	PERIOD (sec)	HORIZONTAL REACTION (kN) BETWEEN DECK & SUPPORT IN X-DIRECTION											Σ_1^{11}	MAX. INDIVIDUAL PIER BASE MOMENT (kN.m)
				1	2	3	4	5	6	7	8	9	10	11		
	307	1	5,434				1523	1547	1770	3508					8348	195 200
	232	1	3,523						1324	2610	10080				14014	354 300
	237	1	3,403					1286	1372	2656	10270				15584	361 200
	240	1	3,294				1223	1251	1495	2682	10380				17031	365 400
	227	1	2,884			4696	1155	1187	1443	2531	9861				20873	347 600
	135	1	2,106							1443	5636	14980			22059	374 500
	133	1	2,082						991	1423	5567	14800			22781	370 000
	131	2	2,059					944	1006	1404	5500	14630			23484	365 700
	118	2	1,923			2465	816	851	1094	1255	4958	13220			24659	330 600
	70	2	1,392			1490	756	754	886	687	2781	7233	13270		27857	265 500
	59	3	1,092		12580	1106	672	698	850	534	2374	6315	11660		36789	251 700
	236	1	3,129				3271	3402	3511	7603					17787	241 200
	145	1	2,186						1909	5176	15250				22335	319 600
	135	2	2,098					1813	1903	4780	14220				22716	298 200
	127	2	2,019				1708	1765	1721	4476	13340				23010	279 900
	68	2	1,403							2083	7435	15360			24878	237 600
	67	2	1,382						767	2145	7338	15230			25480	235 600
	60	2	1,254			3358	800	848	708	1894	6672	13890			28170	215 100
	41	4	0,763		18690	2720	333	548	322	1163	4674	10810	16190		55450	242 500

NOTE Where no horizontal reaction value is shown the support is assumed to be frictionless
P denotes a "pinned" bearing
F denotes a pier integral with the deck

14.3.2 Piers integral with deck

Only one configuration of fixed (integral) and sliding connections was computed. There were no releases at the pier tops and the abutment connections were released for X-translation, Y-rotation and Z-rotation. The forces and moments are the figures given in brackets in table 14.5

14.4 Z-Excitation

The configuration computed for vertical excitation was the one described in 14.3.1 above with pier tops pinned for longitudinal movements. Based on Housner[1,2]'s view, stated in chapter 2, the vertical accelerations were taken as having 0,60 times the value of the horizontal accelerations. The moments and forces are given in table 14.6.

TABLE 14.5 : Y-EXCITATION : MOMENTS AND SHEARS IN DECK AND SUPPORTS

SUPPORT NODE NO.	1	2	3	4	5	6	7	8	9	10	11
Horizontal Bending Moment in deck (kNm)	0 (0)	84990 (89530)	99040 (102000)	89740 (87560)	124400 (120200)	96710 (99320)	95190 (89280)	74660 (67430)	38290 (35310)	23090 (19520)	0 (0)
Torsion Moment in deck (kNm)	10350 (10280)	16430 (15770)	14290 (13690)	11770 (11350)	5190 (4908)	14460 (13800)	17550 (16810)	13910 (13590)	7264 (7059)	6431 (6548)	6431 (6548)
Transverse horiz-ontal deck-pier reaction (kN)	1717 (1529)	5516 (5497)	3306 (3201)	1495 (1439)	2264 (2175)	1835 (1767)	2614 (2540)	4014 (3948)	5744 (5632)	3450 (3550)	336 (268)
Bending Moment at pier top (kNm)	0 (0)	12920 (12410)	12530 (12100)	4915 (4664)	16790 (16100)	9998 (9602)	10270 (9900)	14290 (13780)	14970 (14450)	4896 (5002)	0 (0)
Bending Moment at pier base (kNm)	0 (0)	107800 (107300)	146500 (142100)	126200 (122200)	175700 (169700)	148800 (144100)	146400 (142600)	137800 (135700)	133200 (130800)	67530 (69130)	0 (0)

NOTE: Figures in brackets refer to integral deck/pier connections.
Figures not in brackets refer to pinned deck/pier connections.

TABLE 14.6 : Z-EXCITATION : MOMENTS AND SHEAR FORCES IN DECK AND SUPPORT REACTIONS

NODE	BENDING MOMENT IN VERTICAL PLANE (kNm)	SHEAR FORCE IN DECK (kN)		SUPPORT REACTION (kN)
		LEFT OF NODE	RIGHT OF NODE	
1	0	-	16	16
21	375			
2	375	1	38	39
22	832			
3	161	22	38	19
23	1051			
4	171	38	24	21
24	857			
5	365	38	10	45
25	381			
6	437	25	25	53
26	391			
7	358	10	38	42
27	852			
8	164	24	37	19
28	1033			
9	157	38	22	18
29	820			
10	370	38	1	38
30	370			
11	0	15	-	15

CHAPTER 15

DISCUSSION OF RESULTS

15.1 Comparison between manual calculation and computer analysis

The results of the computer and manual analysis for longitudinal excitation are given in table 15.1

TABLE 15.1 : COMPARISON BETWEEN MANUAL AND COMPUTER ANALYSIS

	Period in seconds for	
Example No.	1	2
a) Description of condition	Deck pinned to all piers and sliding at abutments	Deck pinned to piers at nodes 6, 7 and 8 and sliding at all other supports
b) Manual calculation ignoring mass of piers	0,938	3,170
c) Manual calculation including effect of pier mass by Rayleigh's method	1,007	3,400
d) Computer analysis	1,092	3,523
Deviation of (d) from (c)	8,4%	3,6%

The agreement between the periods calculated by the manual method and the computer analysis is well within acceptable accuracy, particularly for preliminary calculations. This is very useful because it means that, with a selected response spectrum, the displacements and forces can be obtained very rapidly by a hand calculation with sufficient accuracy to enable the designer to test the effects of trying out different configurations without having to spend time and money on repeated computer runs. In this way the most likely configuration can be determined by the rapid hand method. The selected structural system can then be submitted to a computer analysis to obtain a more accurate set of displacements, forces and moments upon which to base the design.

15.2 Comparison between longitudinal (X-) and lateral (Y-) motions

Table 15.2 gives selected results in the directions of the X- and Y- reference axes, showing the general relationship between the magnitudes of the displacements and forces in these directions.

In responding to longitudinal excitation, the high axial stiffness of the deck causes all the connected pier-tops to displace by the same amount and the total force so generated is distributed among the piers in proportion to their bending stiffnesses. The short piers are much stiffer than the long ones and, when connected to the deck, they carry a very high proportion of the force required to accelerate the mass of the whole deck along its axis. This accounts for the high value of 18690 kN for "maximum individual deck-pier reaction" under the X-excitation column in table 15.2. Significantly, the highest pier base moments occur in the shorter piers rather than in the longer ones.

In responding to transverse excitation the piers, acting as vertical cantilevers are much stiffer than the deck acting as a horizontal beam. To illustrate this, compare the horizontal force required to displace the longest (least stiff)

TABLE 15.2 : COMPARISON BETWEEN RESULTS IN 2 REFERENCE DIRECTIONS

Result for	Units	Excitation Direction	
		X	Y
(i) Maximum displacement of deck for case; all piers pinned	m	0,059	0,199
(ii) Max. displacement of deck from all configurations	m	0,307	0,199
(iii) Max. values of sum of deck support reactions (all configurations considered)	kN	55 450	30 238
(iv) Max. individual deck support reaction (all configurations considered)	kN	18 690	5 744
(v) Max. individual pier base moment	kNm	374 000	175 700

pier laterally by 1 metre at its top with the single transverse point load required to produce 1 metre displacement in the deck spanning 600 metres with fixed ends.

The assumption of end-fixity is inspired by reference to the displacement in mode 1, figure 14.2, in which the displaced shape is similar to that of a fixed-ended beam. The cause of the high degree of fixity is the restraint against transverse movement offered by the abutments and the short piers near the ends of the deck.

Pier displacement $\frac{Ph^3}{3EI} = 1{,}000$

$$\therefore p_p = \frac{1 \times 3 \times 30 \times 10^6 \times 50{,}8}{75^3}$$

$$= 10837 \text{ kN}$$

Deck displacement $\frac{Pl^3}{384EI} = 1{,}000$

$$\therefore p_d = \frac{384 \times 30 \times 10^6 \times 156{,}4}{600^3}$$

$$= 8336 \text{ kN}$$

The force required to displace one of the least stiff piers by 1 metre exceeds the force required to displace the deck by 1 metre at its mid length.

Due to its flexibility, the deck more readily follows the different displacements of individual piers than it does in longitudinal motion and, as a result, there is less concentration of acceleration forces on the short stiff piers. This is why the maximum individual deck-pier reactions are so much lower in the transverse motion.

15.3 Vertical (Z-) motion

In the vertical direction the piers have a high axial stiffness and the deck has a high bending stiffness in relation to the span between piers. The axial strains in the piers are so low that the effect of the earthquake on the deck during vertical

excitation is virtually the same as the effect would have been if the deck had been supported on flat ground by short stub piers at the same spacing. Thus the valley shape and the variation in the lengths of piers do not affect the deck response significantly and the vibration modes are all symmetric or asymmetric.

The results obtained for displacements, moments and forces as given in tables 14.3 and 14.6 and in figure 14.3 are very low compared with the results in directions X and Y. These are believed to be grossly incorrect and the error is thought to have arisen due to the scale factor of 0,6 having been inadvertently entered as a direction factor for Z-excitation. It has not been possible to re-run the SAP IV program to correct this error as the program has been corrupted by a hardware fault.

An examination if the output does suggest that it is only the response spectrum analysis which is at fault, the preceding output including mode periods and shapes being valid.

In order to obtain some useful results from the analysis the mode shapes were examined and one was selected to be used as an approximation of the deflected shape for use in a Rayleigh calculation as follows:

With reference to figure 14.3, consider the shape of the deflected span between nodes 3 and 4 in mode number 7. Since both adjacent spans undergo a similar displacement of opposite sense, the moment at support nodes 3 and 4 will be close to zero and the motion will be similar to that of a simply supported span.

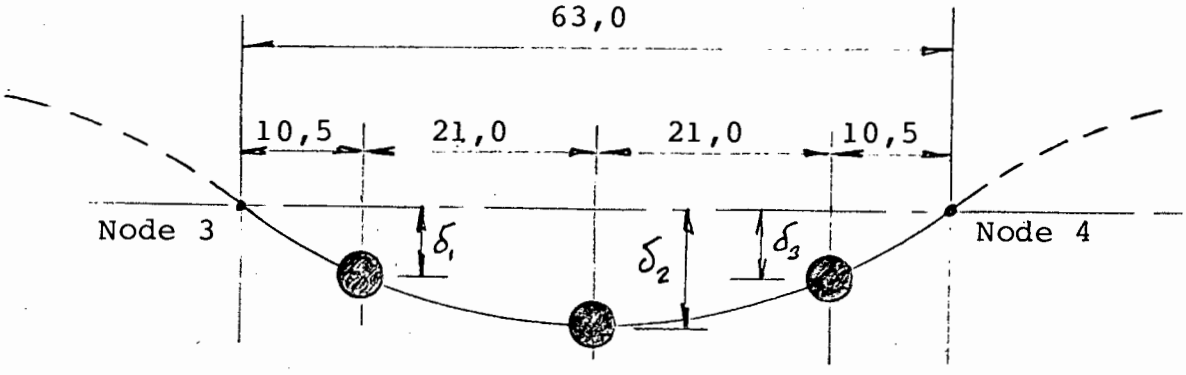

FIGURE 15.1 : EQUIVALENT MASS AND DISPLACEMENT OF 1 SPAN

Total mass of span = 26 x 63 = 1 638 tonne

Consider mass to be lumped as shown in figure 15.1 at 3 positions of 546 tonnes each.

Let the deflection under the static loading be δ_1, δ_2 and δ_3

From eqn.(6.13) period $T = 2\pi \sqrt{\dfrac{M_1\delta_1^2 + M_2\delta_2^2 + M_3\delta_3^2}{k_1\delta^2 + k_2\delta_2^2 + k_3\delta_3^2}}$

Under static loading, for each calculated mass, gravitational force = stiffness x displacement

i.e. $Mg = k\delta$

$\therefore \quad k = \dfrac{Mg}{\delta}$

Thus $T = 2\pi \sqrt{\dfrac{M_1\delta_1^2 + M_2\delta_2^2 + M_3\delta_3^2}{M_1g\delta_1 + M_2g\delta_2 + M_3g\delta_3}}$

since $M_1 = M_2 = M_3$

$$T = 2\pi\sqrt{\frac{\delta_1^2 + \delta_2^2 + \delta_3^2}{g(\delta_1 + \delta_2 + \delta_3)}}$$

Under a UDL of 26 tonnes/m, the midspan deflection

$$= \frac{5\omega l^4}{384EI}$$

$$\text{i.e. } \delta_2 = \frac{5 \times (26 \times 9{,}81) \times 63^4}{384 \times 30 \times 10^6 \times 21{,}7}$$

$$= 0{,}08036 \text{ m}$$

$$\text{and } \delta_1 = \left[1 - \left(\frac{2}{3}\right)^2\right] \delta_2$$

$$= 0{,}55556\ \delta_2$$

$$= 0{,}0446 \text{ m}$$

$$\text{Thus } T = 2\pi\sqrt{\frac{0{,}0446^2 + 0{,}08036^2 + 0{,}0446^2}{9{,}81\ (0{,}0446 + 0{,}08036 + 0{,}0446)}}$$

$$= 0{,}4977 \text{ secs}$$

(This compares favourably with the period for mode 7 obtained from the computer : 0,474 secs)

Now from figure 9.2, with T = 0,5 secs.

acceleration (a) = 0,5g

Applying the scale factor of 0,6 for vertical excitation, take a = 0,5g x 0,6

$$= 0{,}3g$$

Forces acting on the masses during vibration are thus:-

$F_1 = 546 \times 0,3 \times 9,81 \times 0,5556 = 893$ kN

$F_2 = 546 \times 0,3 \times 9,81 = 1607$ kN

$F_3 = 546 \times 0,3 \times 9,81 \times 0,5556 = 893$ kN

These forces produce the following forces and moments in the span concerned :-

$$\text{Midspan bending moment} = 893 \times \frac{63}{6} + 1607 \times \frac{63}{4}$$

$$= 9376 + 25310$$

$$= 34687 \text{ kNm}$$

$$\text{Shear force at end of span} = 893 + \frac{1607}{2}$$

$$= 1697 \text{ kN}$$

By way of comparison the corresponding values due to static loading are :-

$$\text{Midspan bending moment} = 546 \times 9,81 \left\{\frac{63}{6} + \frac{63}{4}\right\}$$

$$= 140\ 601 \text{ kNm}$$

$$\text{Shear force at end of span} = 546 \times 9,81 \times 3 \times 0,5$$

$$= 8034 \text{ kN}$$

Referring again to figure 14.3, consider the spans between nodes 5 - 6 and 6 - 7. It would appear that the maximum curvature at a support position occurs at node 6. As would be expected, therefore, the maximum support moment given by the computer occurs at node 6, the value being 437 kNm. If we compare the computer results (given in figure 14.6) with the results of the foregoing manual calculation for bending moment at the midspan between nodes 3 and 4 we obtain a factor :

$$\frac{\text{Manual value}}{\text{computer value}} = \frac{34687}{1051} = 33$$

Applying this factor to the support moment at node 6 we obtain a bending moment of 437 x 33 = 14 423 kNm. Similarly, the maximum computed support reaction of 53 kN at node 6 is factored up to 53 x 33 = 1749 kN.

15.4 Effect of parameter changes on longitudianl (X-) responses

15.4.1 Piers pinned to deck

Table 14.1 shows the longitudinal displacements as well as the corresponding mode number and period of vibration for each of a series of combinations of pinned and sliding bearings between deck and supports.

In each configuration the deck mass is the same but the total mass of piers participating in the motion depends on how many piers are pinned to the deck. The effect of the pier mass is relatively low however (see chapter 9). It can therefore be said that the system mass varies very little from one configuration to another. The combined stiffness of the pinned piers, on the other hand, varies very considerably depending on which piers are pinned.

Since the period $T = \frac{2\pi}{\omega} = 2\pi\sqrt{\frac{M}{K}}$

it is clear that the larger the stiffness K, the lower the period T. This is very clearly borne out by table 9.1 in which the shorter piers have very much higher stiffness than the longer ones.

The forces and moments corresponding to the various configurations are shown in table 14.4.

In any one configuration, each pinned pier displaces the same amount and the force at its top = displacement x stiffness. Thus the shorter stiffer piers carry more of the force required to accelerate the deck than the longer ones.

In comparing one configuration with another it is important to remember that the force required to accelerate the deck is related to the amplitude of the vibration and to the period of the vibration. An increase in amplitude for a given period implies increased acceleration. Alternatively, a decrease in period for a given amplitude will also imply increased acceleration.

TABLE 15.3 : COMPARISON BETWEEN CASES 1 AND 8 IN TABLE 14.4

Case	Displacement (m)	Period (sec)	P (kN)	System Mass (tonnes)	Combined Pier stiffness kN/m
1	0,307	5,434	8348	16828	25542
8	0,131	2,059	23484	16762	189824

Although the displacement in 1 is so much greater than in 8, the force P is actually much less. This is because of the increased stiffness of 8 which leads to a much shorter period and a higher acceleration. There is very little difference in the participating mass between 1 and 8.

15.4.2 Piers integral with deck

Table 14.4 shows the translational and rotational displacements, as well as the corresponding mode number and period of vibration for each of a series of combinations of piers cast integral with the deck and piers having sliding bearings.

As in the case of pinned piers in 15.4.1 the greater the stiffness K, the smaller the period T and the smaller the displacements. The forces and moments corresponding to the various configurations are given in table 14.4. Apart from the extremely high and extremely low stiffness

cases, there is not a great variation in P between the different configurations despite fairly large differences in displacement and period.

For any pinned configuration it is found that the corresponding integral configuration, with its increased stiffness, leads to decreased displacements and decreased periods but to greater values of P. With one exception the maximum individual pier base moments are all reduced by making the piers integral with the deck.

TABLE 15.4 : COMPARISON BETWEEN INTEGRAL AND PINNED CONNECTIONS

Configuration	Displacement (m)	Period (secs)	ΣP (kN)	Maximum individual pier base moment (kNm)
4-5-6-7. (P)	0,307	5,434	8348	195200
(F)	0,236	3,129	17787	241200
6-7-8. (P)	0,232	3,523	14014	354300
(F)	0,145	2,186	22335	319600
5-6-7-8. (P)	0,237	3,403	15584	361200
(F)	0,135	2,098	22716	298200
6-7-8-9. (P)	0,133	2,082	22781	370000
(F)	0,067	1,382	25480	235600
4-5-6-7-8. (P)	0,240	3,294	17031	365400
(F)	0,127	2,019	23010	279900
3-4-5-6-7-8-9. (P)	0,118	1,923	24659	330600
(F)	0,060	1,254	28170	215100
2-3-4-5-6-7-8-9-10. (P)	0,059	1,092	36789	251700
(F)	0,041	0,763	55450	242500
7-8-9. (P)	0,135	2,106	22059	374500
(F)	0,068	1,403	24878	237600

15.4.3 Summary of longitudinal (X-) responses

A study of the effects of the parameter changes makes the following observations possible:-

(i) The configurations involving integral piers and those involving pinned piers all belong to a progression of systems in which the responses are related to the overall stiffness.

(ii) The stiffer the system the shorter the period.

(iii) Period increases with displacement.

(iv) Period decreases with increase in P in a manner which is nearly linear except for configurations which involve the short stiff piers closest to the abutments. When these are included there is a sharp increase in the value of P as the period decreases further.

(v) It is evident that the maximum individual pier base moment is fairly constant in the period range of about 2 seconds to 3,5 seconds. An increase in period above 3,5 seconds or a decrease in period below 2 seconds results in reduced maximum individual pier base moments. It also appears that a system having integral piers will develop lower maximum individual pier base moments than a pinned system having the same period.

15.4.4 Use of the results for design

The results of the analysis are very helpful in selecting the configuration best suited to the design in hand. The

design criteria would normally be as follows:

(i) Deck displacements in the X-direction should be kept as low as possible in order to minimise cost and complication of bridge bearings and expansion joints. This calls for a short period system.

(ii) It is desirable to avoid high values of P so as to minimise all the pier base moments and thereby also the cost of the piers and the foundations. This calls for a long period system.

(iii) Although we are interested in the maximum individual pier base moment inasmuch as it may govern the pier design and cross section, it will not necessarily be representative of most of the other piers and is not of major interest in selecting the configuration.

(iv) In order to limit axial strains in the deck resulting from temperature, elastic shortening, creep and shrinkage, it is desirable to offer as little restraint as possible. This is best achieved in the systems having the longer periods.

(v) There may be other restraints associated with the assumed method of construction. For example, if the deck is to be built by the "Incremental Launching Method" (i.e. built on one bank and pushed out over the pier tops) it should be assumed that all the piers have bearings rather than being integral with the deck.

In order to satisfy the above requirements in our model, it would appear that we need to find a system with the greatest tolerable displacement and the least restraint against axial strains in the deck. The system best satisfying these requirements is number 2 having pinned bearings at nodes

6, 7 and 8 and a maximum displacement of 232 millimetres due to the assumed earthquake.

15.5 Effects of Parameter Changes on Transverse (Y-) Responses

Table 14.5 shows that the transverse displacement of the deck is only very slightly reduced by making the deck integral at all piers instead of pinned at all piers. In table 15.5, the pinned and integral systems are compared in terms of the forces and moments at the deck/pier connections.

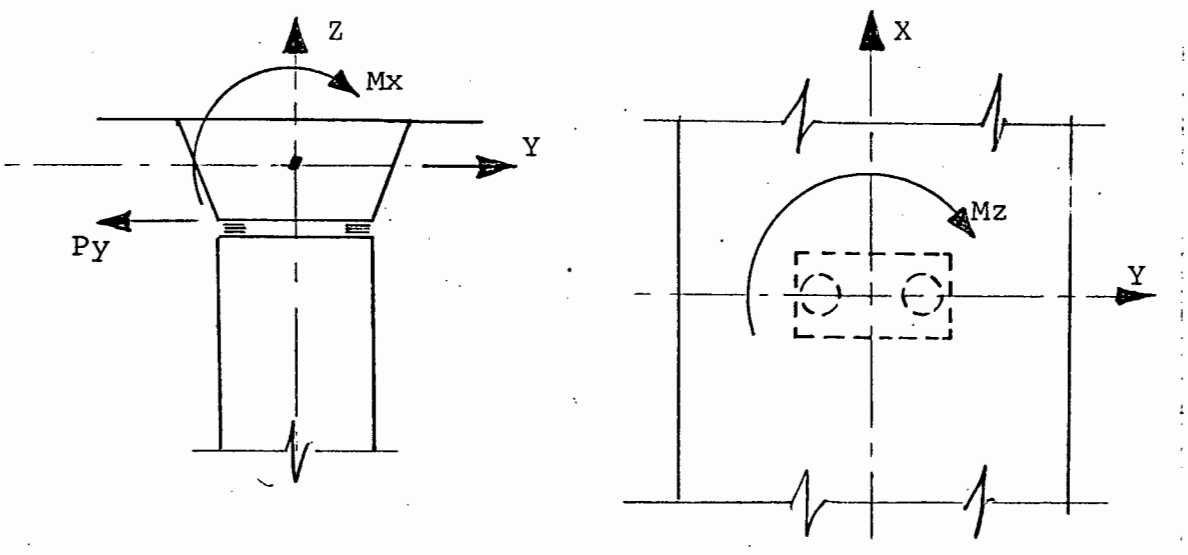

FIGURE 15.2 : FORCES AND MOMENTS AT DECK/PIER CONNECTION

It must be noted that the connection at the top of a "pinned" pier permits the deck to rotate relative to the pier about the Z (vertical) and Y (transverse) axes but not about the X (longitudinal) axis. The resistance to X-rotation is achieved by means of a couple acting via the bearings shown in figure 15.2.

TABLE 15.5 : TRANSVERSE MOMENTS AT PIER BASES FOR PINNED AND FIXED CONNECTIONS

Member and Node	M x		P y		M z	
	Pinned	Fixed	Pinned	Fixed	Pinned	Fixed
21 , 2	12929	12410	5516	5497	0	14080
23 , 3	12530	12100	3306	3201	0	15950
25 , 4	4915	4664	1495	1439	0	11030
27 , 5	16790	16100	2264	2175	0	4096
29 , 6	9998	9602	1835	1767	0	9062
31 , 7	10270	9900	2614	2540	0	14600
33 , 8	14290	13780	4014	3948	0	13630
34 , 9	14970	14450	5744	5632	0	7000
35, 10	4896	5002	3450	3550	0	5986

It is evident that making the deck integral with the piers holds no benefit as far as transverse (Y) excitation is concerned. The displacements, as well as the moment Mx and the force Py are hardly affected whereas the creation of integral joints causes torsion moments to be set up in the piers. It would seem more advantageous therefore to make the connections pinned.

CHAPTER 16

NUMBER OF MODES REQUIRED IN ANALYSIS

In performing a response spectrum analysis on a multi-degree-of-freedom system it is necessary to decide how many vibration modes are to be considered. Clough[6] has the following observation:

"In general, the lower modes make the principal contributions to the response and good approximations can frequently be obtained by considering only the first few modes in the analysis. On this basis the best single-degree-of-freedom approximation generally is obtained by considering only the first mode contribution".

This view is borne out by the results obtained in the analysis. Excitations in the X, Y and Z directions were each analysed for 12 modes. In each case the lowest mode relative to the direction being considered accounted for the dominant part of the motion. This can be seen by referring to tables 14.1, 14.2 and 14.3 showing the displacements. The following is an extract from tables 14.1, 14.2 and 14.3 and shows the proportion of the maximum displacement for 12 modes accounted for by the lowest mode.

TABLE 16.1 : PROPORTION OF DISPLACEMENT ACCOUNTED FOR BY LOWEST MODE

Excitation direction	Uncoupled modes participating	Maximum displacement for 12 modes combined (m)	Corresponding displacement for lowest mode (m)	Proportion %
X	3,8,9,10	0,059	0,059	100
Y	1,2,4,5,11	0,199	0,198	99,5
Z	6,7,12	0,00051	0,00051	100

If displacements other than the maximum values are of interest, it appears to be necessary to investigate some modes other than the lowest. This can be seen by examining the displacements in the 2nd, 4th, 5th and 11th modes for Y-excitation and the displacements in the 12th mode for Z-excitation.

Since the computer time required to carry out a response spectrum analysis such as the foregoing is not seriously lengthened by including multiple modes, it is considered worthwhile doing at least one run in each excitation direction with up to 12 modes. In any case it is not obvious in advance of the analysis which mode is to be the lowest for the direction being considered. As shown in table 16.1, the lowest mode for X-excitation was found in the 3rd mode while the lowest mode for Z-excitation was found in mode number 7. 12 modes would therefore seem to be a suitable number of modes to investigate in this type of analysis.

CHAPTER 17

COMPARISON BETWEEN EARTHQUAKE LOADING AND OTHER LOADING ON THE MODEL

The magnitude of the forces induced by the selected earthquake are compared with the forces induced by other loadings in the following tables:

TABLE 17.1 : LOADING ALONG AXIS OF DECK (X-DIRECTION)

	Earthquake loading (kN)	Traction/ braking force (kN)
Pinned at abutment only	50502	400
Pinned at nodes 4-5-6-7	8348	

TABLE 17.2 : TRANSVERSE LOADING (Y-DIRECTION)

	Earthquake loading	Wind loading
Maximum horizontal bending moment in deck (kNm)	124 400	75400

TABLE 17.3 : VERTICAL LOADING (Z-DIRECTION)

	Earthquake loading**	Structural dead load	Traffic live load
Maximum midspan moment in deck (kN)	34687	4960	42 210
Maximum support moment in deck (kNm)	14423	138900*	37430
Maximum individual support reaction	1749	18270	6730

* Negative moment predominates due to balanced cantilever method of construction.

** Adjusted values as per 15.3

In bridges such as that represented by the model, the vertical loading consists of gravitational forces acting on the dead-mass and on the live-mass and inertia forces due to earthquake acceleration. The gravitational loads are equal to mass x g whereas the earthquake loads are equal to mass x a proportion of g, the value seldom exceeding 0,5g. Thus it is to be expected that the earthquake loading will represent only a fraction of the total vertical loading. This is confirmed by table 17.3

In the transverse direction gravity plays no part in the loading and it is interesting to note in table 17.2 that the effects of wind are comparable with those of the selected earthquake.

In the longitudinal direction the traction/braking forces for this model are very much smaller than the earthquake effects.

CHAPTER 18

DESIGN OF STRUCTURAL CONFIGURATION TO CONTEND WITH SEISMIC LOADING IN VIADUCT BRIDGES

It is considered worthwhile mentioning some of the factors other than earthquake loading which should be taken into account when selecting the most suitable arrangement of deck-pier connections for a viaduct-type structure. The configuration selected will normally be a compromise between various different configurations, each of which may be an optimum for a particular loading or displacement parameter viewed in isolation. The following are the main points to be considered:

18.1 Axial Strains in Deck

It is necessary to determine the amounts of lengthening or shortening which are expected to take place in the deck due to temperature, elastic shortening, creep and shrinkage, excluding any effects which may have occurred whilst the structural element concerned was in a temporarily free condition during construction.

18.2 Selection of Point of Fixity

The deck may be secured in position for longitudinal movement in a number of different ways. One common way is to attach the deck to one abutment by means of pinned bearings. This would force the deck to undergo exactly the same movements as the ground. The structural stiffness for longitudinal movements of the deck would approach infinity and this would be associated with a very low period of oscillation. At the low-period end of the response spectrum there would be no amplification of ground acceleration but on the other hand the acceleration of the structure could not reduce below that of the ground as would have been the case with a flexible, long period structural arrangement. As a result, high forces would develop between deck and abutment. Alternatively, one or more of the piers may be pinned or integrated with the deck whilst permitting sliding at the abutments. This will generally be a more flexible

arrangement than pinning at an abutment and larger translations will have to be accommodated although the horizontal inertia forces will be lower. If more than one pier is pinned to or integral with the deck, the axial strains referred to in 18.1 will set up horizontal forces at the pier tops. In practice, even the sliding bearings generate horizontal forces as they are not fully frictionless. From this point of view, it is desirable to have non-sliding connections at as few pier tops as possible.

18.3 Longitudinal Live Loads

Acceleration, braking and wind loads apply horizontal forces to the substructure at the non-sliding supports. When these forces are taken on piers it is necessary to ensure that sufficient piers are connected to the deck to keep the live load forces and bending moments in the piers down to acceptable levels.

18.4 Displacements

The structure is required to be stiff enough to prevent longitudinal displacements from becoming unmanageable as far as bearings, expansion joints and services are concerned. Additional stiffness may be achieved, if needed, by connecting more piers to the deck, the shorter piers being more effective in this regard.

18.5 Constraints Dictated by the Construction Method

The type of connection between the deck and piers may be dictated partly or wholly by the method of construction. For example, certain types of "balanced free cantilever" construction require all deck/pier connections to be fully integral. Alternatively, a deck placed by means of the "Incremental Launching" method may require all piers to have sliding bearings.

CHAPTER 19

GENERALISATIONS ABOUT OTHER BRIDGES

The techniques illustrated in this work can be readily applied to other types of bridges in which the separate modes of vibration can be identified and computed.

Bridges falling into this category would include most road-over-road grade separation bridges as well as river crossings in which the bridge deck is carried on a number of piers.

From the foregoing work, it would appear that the following generalisations can be made in respect of such bridges:-

19.1 Longitudinal Excitation

Any deck which is attached to the ground via an inflexible support, such as a very stiff abutment, will be forced to move with the ground and will be subjected to an inertia force equal to the deck mass x ground acceleration. In cases where the deck is not connected to inflexible supports, but is attached to the piers, the pier lengths become significant. Where the piers are short (i.e. approximately 6m as for grade separation or low level river crossings) they will be fairly stiff and lead to periods of vibration in the range of approximately 0,2 seconds to 1 second.

With reference to figure 9.2, it will be seen that most of this range coincides with that in which the ground motion has its maximum acceleration values and in which the largest amplifications occur. From figure 9.2 it is evident that accelerations of up to 1,0g could occur in this range if a damping ratio of 0,02 is assumed.

19.2 Transverse Excitation

Most bridges of the type being considered have piers which have dimensions which are much greater transversely than in the direction of the bridge axis. Consequently their transverse stiffness is much greater than their longitudinal stiffness. For low level bridges as described in 19.1, this transverse stiffness of the supports is almost infinite and the deck is caused to undergo transverse movements the same as those of the ground, leading once more to forces equal to mass x ground acceleration. Although these forces may be fairly high, the moments caused at the bases of the supports will not be excessive due to the short lever arm. The deck itself is normally very stiff in horizontal bending and therefore provides little relief of inertia force resulting from lateral deflection.

19.3 Vertical Excitation

The response of these structures to vertical excitation is related mainly to the stiffness of the deck. The lengths of the piers would not be expected to play a significant part in the vertical movement since they normally possess a relatively high axial stiffness. An exception to this is the case where piers are built integral with a deck oscillating in a mode in which alternate spans have upward and downward displacements. In such a case the bending stiffness of the piers would influence the displacements of the deck.

BIBLIOGRAPHY

1. BOLT, B.A., "Causes of Earthquakes", Earthquake Engineering, (Co-ordinating editor R.L. Wiegel); Englewood Cliffs, N.J. : Prentice Hall, Inc. 1970, p. 21-45.

2. HOUSNER, G.W., "Strong ground motion", Earthquake Engineering, (Co-ordinating editor R.L. Wiegel); Englewood Cliffs, N.J. : Prentice Hall, Inc. 1970, p. 75-91.

3. LAURIE, J.A.P. and PUTTERILL, K.E., "Engineering Implications of Earthquakes in Southern Africa", Pretoria : N.B.R.I., C.S.I.R. Ref. No. R/BOU 340, 1970.

4. NEWMARK, N.M. "Earthquake response analyses of reactor structures", Nuclear Engineering and Design, 20, 303-322, 1972.

5. NEWMARK, N.M. and ROSENBLUETH, E., Fundamentals of Earthquake Engineering, Prentice Hall, 1971.

6. CLOUGH, R.W., "Earthquake response of structures", Earthquake Engineering, (Co-ordinating editor R.L. Wiegel); Englewood Cliffs, N.J. : Prentice Hall, Inc. 1970, p. 307-334.

7. BATHE, K.J., WILSON, E.L. and PETERSON, F.E., "SAP IV : A structural analysis program for static and dynamic response of linear systems", College of Engineering, University of California, 1973.

8. HOUSNER, G.W., "Design Spectrum", Earthquake Engineering, (Co-ordinating editor R.L. Wiegel); Englewood Cliffs, N.J. : Prentice Hall, Inc. 1970, p. 93-106.

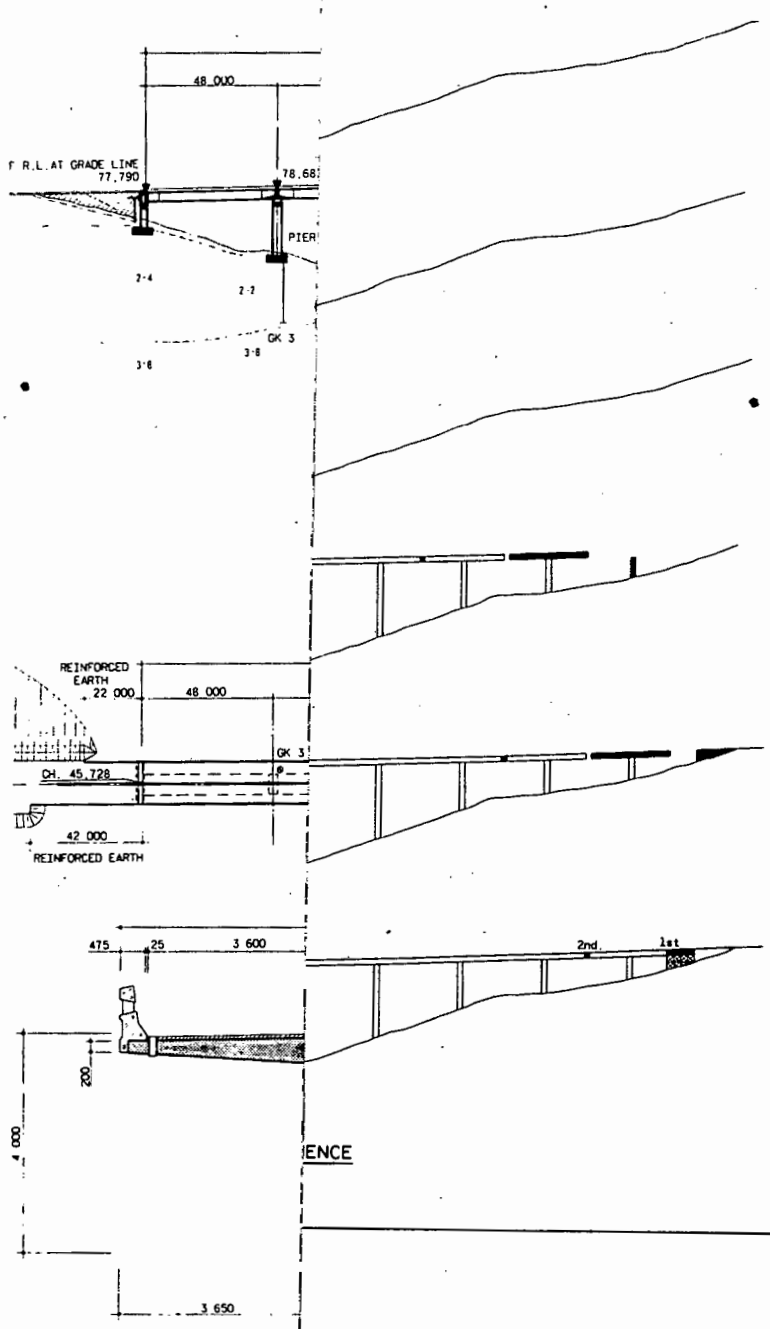

ENCE

400
250
4 000
3 200
400

PPENDIX I

REDUCED DRAWING

0 mm — 100 millimetres on original drawing — 100

REDUCED DRAWING

APPENDIX II

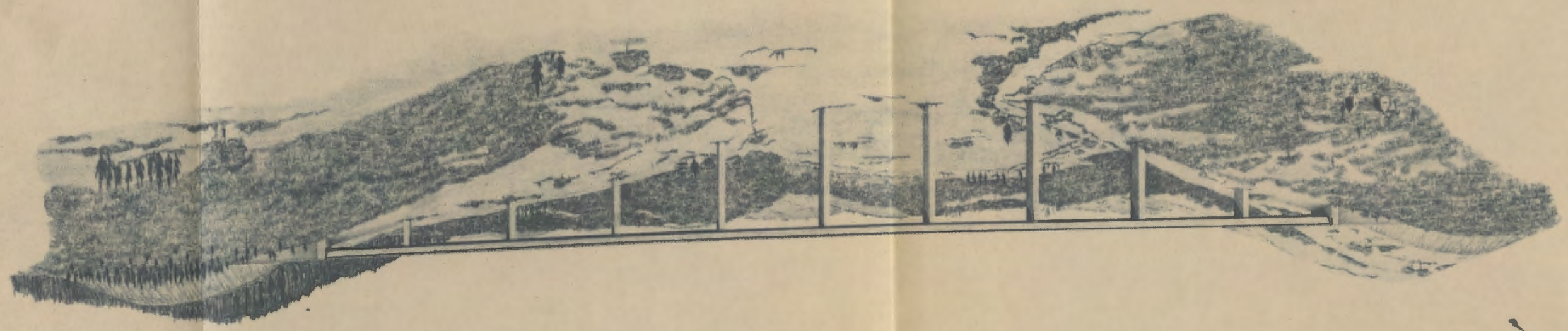

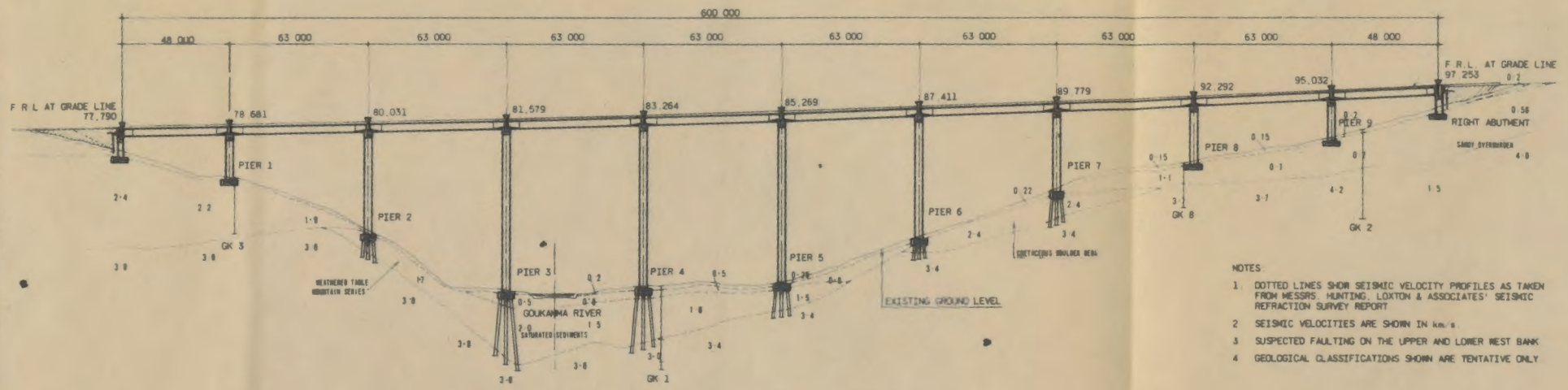

NOTES

1. DOTTED LINES SHOW SEISMIC VELOCITY PROFILES AS TAKEN FROM MESSRS. HUNTING, LOXTON & ASSOCIATES' SEISMIC REFRACTION SURVEY REPORT
2. SEISMIC VELOCITIES ARE SHOWN IN km/s
3. SUSPECTED FAULTING ON THE UPPER AND LOWER REST BANK
4. GEOLOGICAL CLASSIFICATIONS SHOWN ARE TENTATIVE ONLY

LONGITUDINAL SECTION
SCALE: 1:1000

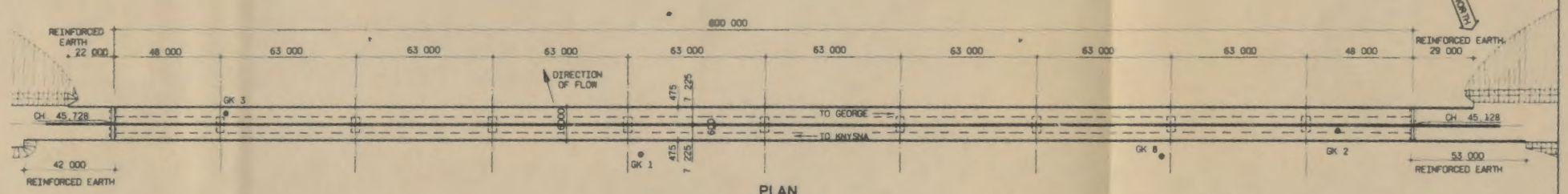

PLAN
SCALE: 1:1000

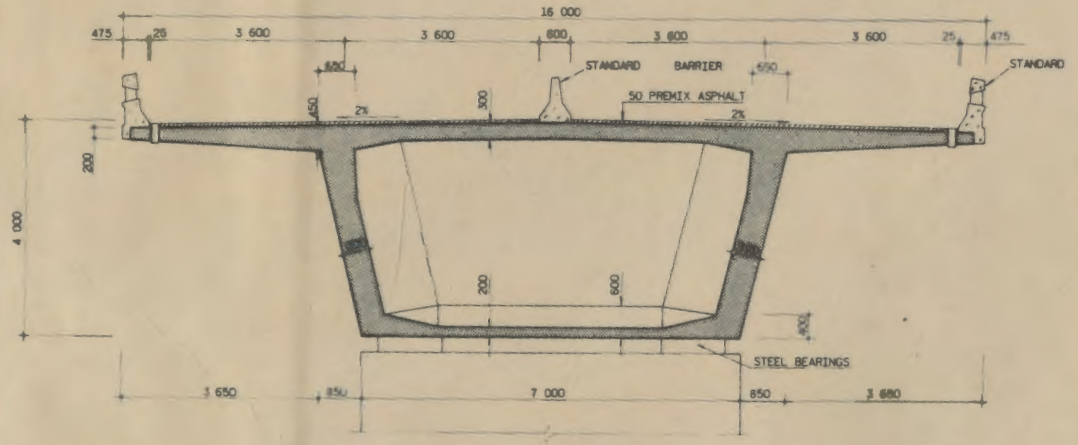

SECTION THROUGH DECK
SCALE: 1:50

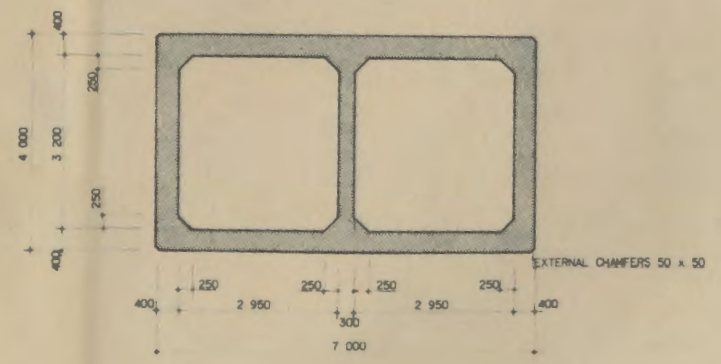

CROSS SECTION THROUGH PIERS
SCALE: 1:50

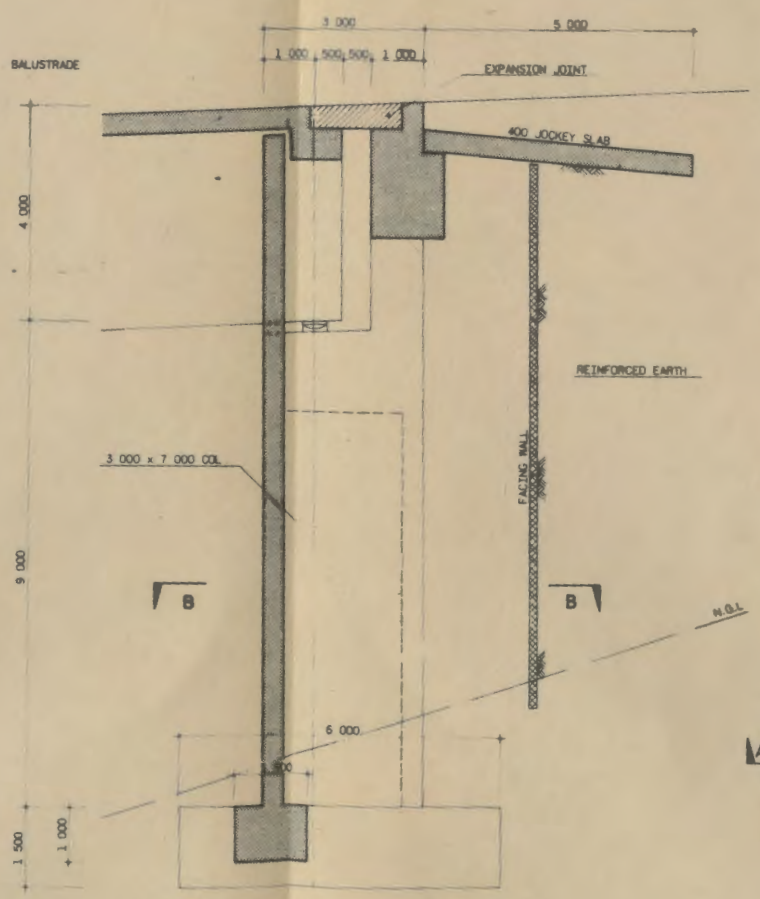

SECTION A-A THROUGH RIGHT ABUTMENT
SCALE: 1:50

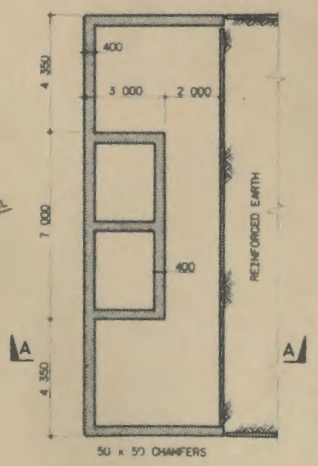

PLAN B-B THROUGH RIGHT ABUTMENT
SCALE 1:100

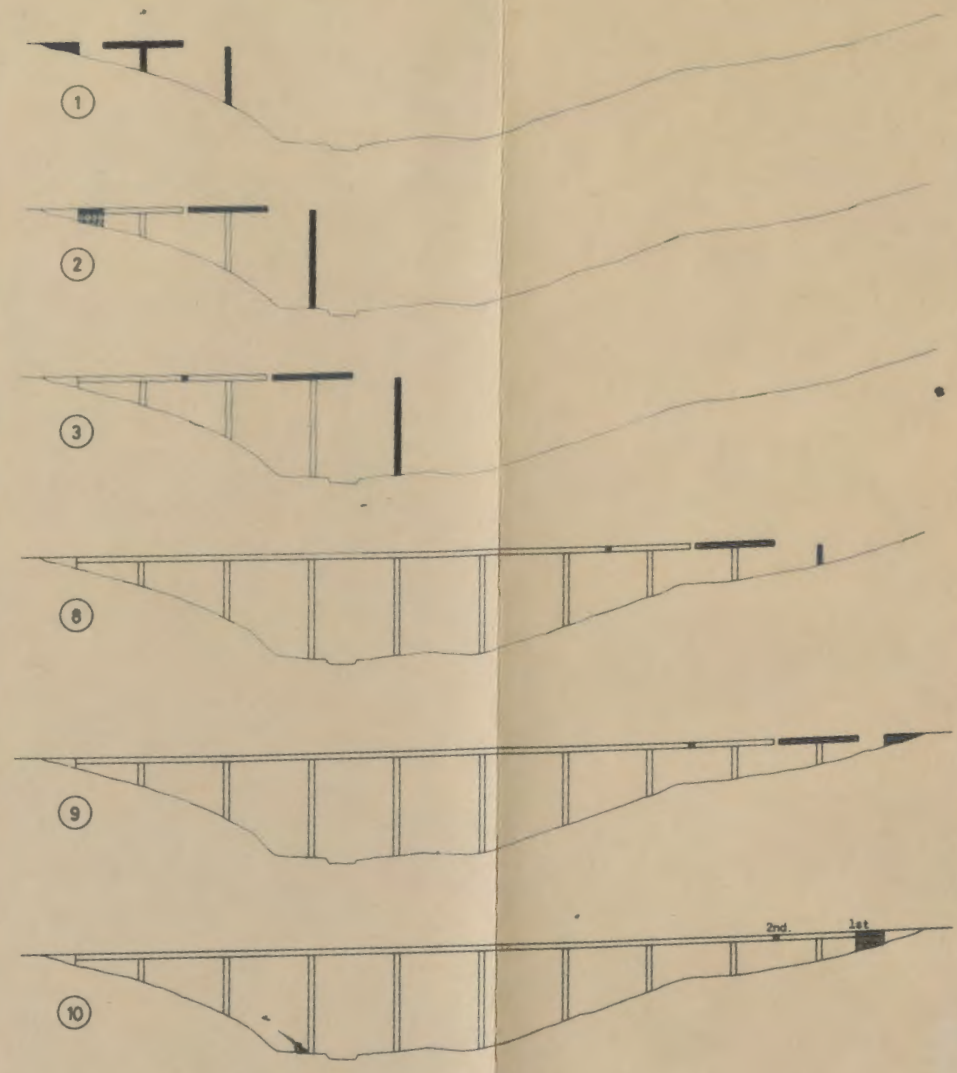

CONSTRUCTION SEQUENCE
SCALE: 1:2000

APPENDIX I

REDUCED DRAWING